刘柄梁,赵正,郭娜欣等. 2026. 攀西力马河镁铁-超镁铁岩浆演化与镍成矿:来自矿物化学的证据. 岩石学报,42(06):2137-2155, doi:10.18654/1000-0569/2026.06.11;CSTR:32089.14.APS-ysxb.2026.06.11

攀西力马河镁铁-超镁铁岩浆演化与镍成矿:来自矿物化学的证据*

刘柄梁[1] 赵正[2]** 郭娜欣[2] 李陈浩[2]

LIU BingLiang[1], ZHAO Zheng[2]**, GUO NaXin[2] and LI ChenHao[2]

1. 桂林理工大学地球科学学院,桂林 541004
2. 自然资源部成矿作用与资源评价重点实验室,中国地质科学院矿产资源研究所,北京 100037
1. *College of Earth Sciences*, *Guilin University of Technology*, *Guilin* 541004, *China*
2. *MNR Key Laboratory of Metallogeny and Mineral Assessment*, *Institute of Mineral Resources*, *Chinese Academy of Geological Science*, *Beijing* 100037, *China*

2025-04-30 收稿, 2026-03-01 改回.

Liu BL, Zhao Z, Guo NX and Li CH. 2026. Ultrabasic magmatic evolution of the Panxi Limahe mafic-ultramafic intrusion and nickel mineralization: Evidence from mineral chemistry. *Acta Petrologica Sinica*, 42(6): 2137-2155, doi: 10.18654/1000-0569/2026.06.11; CSTR: 32089.14.APS-ysxb.2026.06.11

Abstract The Limahe nickel deposit in Huili County, Sichuan Province, is a typical magmatic copper-nickel sulfide deposit in China. Its petrogenesis and mineralization are closely related to the Late Hercynian mantle plume activity on the western margin of the Yangtze Block. However, there is still a lack of consensus regarding the mechanism of nickel enrichment during the evolution of the mafic-ultramafic magma. In this study, electron probe microanalysis and LA-ICP-MS techniques were employed to systematically analyze the chemical compositions of olivine and pyroxene from different lithofacies of the Limahe intrusion, aiming to elucidate the genetic relationship between the magmatic source and evolution processes and nickel enrichment and mineralization. A comprehensive comparison was also made with the petrological and mineralogical characteristics of typical magmatic sulfide deposits in the Panxi region and other parts of China. The results indicate that the parental magma of the Limahe intrusion originated from deep-seated garnet peridotite mantle. Its mafic and ultramafic units exhibit characteristics of tholeiitic and high-Mg basaltic magmas, respectively. During magmatic evolution, the high Li contents in olivine from the Limahe intrusion suggest significant contamination by middle-upper crustal materials, implying that the addition of external sulfur triggered sulfide segregation. The mineralization difference between the Limahe intrusion and the adjacent Guanhe intrusion (which lacks nickel mineralization) is mainly attributed to the stage of sulfide segregation: early segregation in the Limahe intrusion effectively enriched metal elements, leading to the formation of a high-grade deposit; in contrast, late-stage segregation in the Guanhe intrusion resulted only in low-grade mineralization. Therefore, the magmas related to nickel mineralization in this region were primarily derived from deep-seated garnet peridotite mantle, and the addition of crustal sulfur induced sulfide segregation during the early stage of magmatic evolution. The coupling of these conditions and processes constitutes the key controlling factors for the formation of large magmatic copper-nickel sulfide deposits in the Panxi region.

Key words Mineralogy; Magmatic sources; Sulfide segregation; Limahe; Panzhihua-Xichang (Panxi) region

摘 要 四川会理力马河镍矿是我国典型的岩浆铜镍硫化物矿床,其成岩成矿作用与晚海西期扬子西缘地幔柱活动密切相关,然而关于镁铁-超镁铁质岩浆演化过程中镍的富集机制问题尚缺乏统一认识。本研究运用电子探针与LA-ICP-MS技术,系统分析了力马河岩体不同岩相中橄榄石与辉石的化学组成,用以解析岩浆源区和演化过程与镍富集成矿的成因联系,并综合对比了攀西地区及我国典型岩浆硫化物型矿床岩石矿物学特征。研究结果显示,力马河岩体母岩浆源自深部石榴子石橄

* 本文受中国地质调查局地质调查项目(DD202602109204、DD20242254、DD20230203509)、深地国家科技重大专项(2024ZD1001001)、新一轮找矿突破战略行动科技支撑项目(ZKKJ202424)和华锡集团企业项目(HE2506)联合资助.

第一作者简介: 刘柄梁,男,2000年生,硕士生,矿物学、岩石学、矿床学专业,E-mail: 2840195443@qq.com

** **通讯作者:** 赵正,男,1984年生,研究员,博士生导师,主要从事矿床学研究,E-mail: kevin8572@hotmail.com

榄岩地幔,其镁铁单元与超镁铁单元分别具有拉斑玄武质岩浆和高镁玄武质岩浆特征。在岩浆演化过程中,力马河岩体橄榄石高 Li 含量说明其经历了明显的中-上地壳物质混染,推断发生了外源硫触发硫化物熔离。力马河岩体与邻区关河岩体(不含镍矿)的成矿差异主要源于硫化物熔离阶段:力马河岩体为早期熔离,这种早期熔离机制有效地富集了金属元素,促成高品位矿床;关河岩体属晚期熔离,仅致低品位矿化。因此,该区与镍成矿相关的岩浆主要源于深部石榴子石橄榄岩地幔,地壳硫的加入诱发岩浆演化早期硫化物熔离,上述条件与过程的耦合构成了攀西地区大型岩浆铜镍硫化物矿床成矿的关键控制因素。

关键词 矿物学;岩浆源区;硫化物熔离;力马河;攀西地区

中图法分类号 P575.1; P618.63

岩浆铜镍硫化物矿床是全球镍和铂族元素的最主要来源,其成矿作用多与地幔柱活动及深大断裂区岩浆系统相关,主要产出于大火成岩省、克拉通边缘裂谷及造山带伸展区(Naldrett, 2011; Pirajno *et al.*, 2009; 汤中立等, 2011; 李文渊, 2022)。全球铜镍硫化物矿床主要分布于前寒武纪克拉通边缘及其活化带,受控于沟通壳幔的深断裂和古裂谷体系,尤其是在地幔柱与裂谷系统耦合的动力学背景,成矿作用受幔源岩浆演化中硫化物熔体的熔离-侵位过程及硫饱和机制制约(Ross and Travis, 1981; Naldrett *et al.*, 1992; Naldrett, 1999)。我国的铜镍硫化物矿床集中分布于东昆仑造山带、龙首山构造带、中亚造山带和扬子西缘,形成环境多样,如克拉通裂解背景下的幔源岩浆成矿(如金川)(姜常义等, 2015; 莫宣学, 2019),古俯冲带再活化引发的壳幔相互作用成矿(如白鑫滩)(Barnes and Lightfoot, 2005; Pirajno *et al.*, 2009; 汤中立等, 2011; 李文渊, 2015; 赵冰冰等, 2018),以及典型的地幔柱成因大火成岩省成矿(如攀西力马河)。

岩浆铜镍硫化物矿床的成因一直是矿床学研究热点,早期基于 Sudbury 等矿床研究建立了层状侵入体接触带控矿模型(Faggart *et al.*, 1985; 汤中立等, 2006),并应用于 Bushveld 等低品位矿床的勘查(Maier *et al.*, 2001);随着金川和 Noril' sk 等高品位矿床的发现,建立了通道型岩浆硫化物熔体贯入等新成矿模型(Naldrett, 1999; Evans-Lamswood *et al.*, 2000; Maier *et al.*, 2001)。目前,关于岩浆铜镍硫化物矿床中岩浆源区、岩浆演化与成矿的决定性因素尚未明确,如陶琰等(2007)认为攀西地区岩浆铜镍硫化物矿床源区为与高钛玄武质岩浆,而李莹(2010)认为是镍矿相关的镁铁单元与超镁铁单元具有不同的岩浆源区;张飞飞(2023)认为夏日哈木为代表的铜镍硫化物矿床中分离结晶作用并非控制成矿作用的主要因素,而鲍坚(2024)认为其母岩浆在深部发生结晶分异之后发生了多期侵位导致镍富集。

力马河铜镍硫化物矿床位于四川会理,始建于 1958 年,是我国自主建设和正规化开采的首座镍矿山。矿山历经数十年开采,浅部高品位镍矿资源消耗殆尽,深部资源情况不明,成岩成矿关系不清,矿山资源和地区经济发展均面临瓶颈。姚家栋(1988)基于力马河矿床地质特征及岩相学研究,提出深部岩浆熔离贯入模型。Zhang *et al.* (2009)和李莹(2010)从相平衡分析及硅饱和程度角度推断力马河铜镍硫化物矿床为多来源岩浆成矿。陶琰等(2007)通过年代学研究,认为力马河铜镍硫化物矿床为晚海西期峨眉地幔柱活动产物,其岩浆源区具有高钛玄武质岩浆特征。本文以力马河岩体中橄榄石和辉石为窗口,开展精细矿物学研究,揭示不同岩相端元的原始岩浆成分,探讨力马河岩体的岩浆源区与演化、硫化物熔离过程,综合对比区域上成铜镍矿与不成铜镍矿岩体的矿物学特征,为力马河式铜镍硫化物矿床成因提供理论依据。

1 成矿地质背景

攀西地区构造上位于扬子板块西缘,元古宙以来经历了多旋回构造岩浆事件,尤以晚二叠世至早三叠世地幔柱活动引起的镁铁-超镁铁岩浆喷出-侵位作用影响最为广泛(图 1; Lo *et al.*, 2002; 何斌等, 2003; Shellnutt and Zhou, 2007)。区内巨厚的溢流玄武岩喷发和同期的大量镁铁-超镁铁岩层状岩体侵入,构成了一个完整的幔源岩浆作用成矿系统(Xiao *et al.*, 2004)。攀西地区主要产出钒钛磁铁矿、铜矿、铜镍硫化物矿、铜镍铂族元素矿等矿产,其中,钒钛磁铁矿矿床以高钛玄武岩及相关的层状岩体(如攀枝花、红格、白马岩体)为主,铜镍硫化物矿床以遭受强烈地壳混染的低钛玄武岩及一系列小型岩体(如杨柳坪、力马河、金宝山岩体)为标志(Zhou *et al.*, 2008)。攀西地区自晋宁期、加里东、海西期、印支期-喜山期岩浆活动频发,产出镁铁-超镁铁岩、酸性岩和碱性岩。攀西地区岩浆岩和矿床分布明显受断裂构造控制,主干断裂为 NS 向,以金河-箐河断裂、攀枝花断裂、昔格达断裂、安宁河断裂等数条近 NS 向深大断裂为主体,次级断裂为 NE、NW 和 EW 向(张云湘, 1982; 骆耀南, 1985; 蔡文昌, 2021)。主、次级断裂共同构成了攀西地区控岩控矿构造带(李佑国, 2007)。出露地层涵盖下元古界至新生界,共同构成结晶基底的康定群与会理群为区内最古老地层(李宏博, 2012; 骆文娟, 2013)。

攀西地区独特的地质历史孕育了两类世界级的矿床:与高钛岩浆演化相关的钒钛磁铁矿氧化物矿床和与低钛岩浆经地壳混染后形成的岩浆铜镍硫化物矿床(Zhong *et al.*, 2005; Zhou *et al.*, 2008)。矿产主要为钒钛磁铁矿矿床、岩浆铜镍硫化物矿床和稀土矿床(Zhou *et al.*, 2005; Pang *et al.*, 2010; Luan *et al.*, 2014)。晋宁期镁铁质-超镁铁质侵

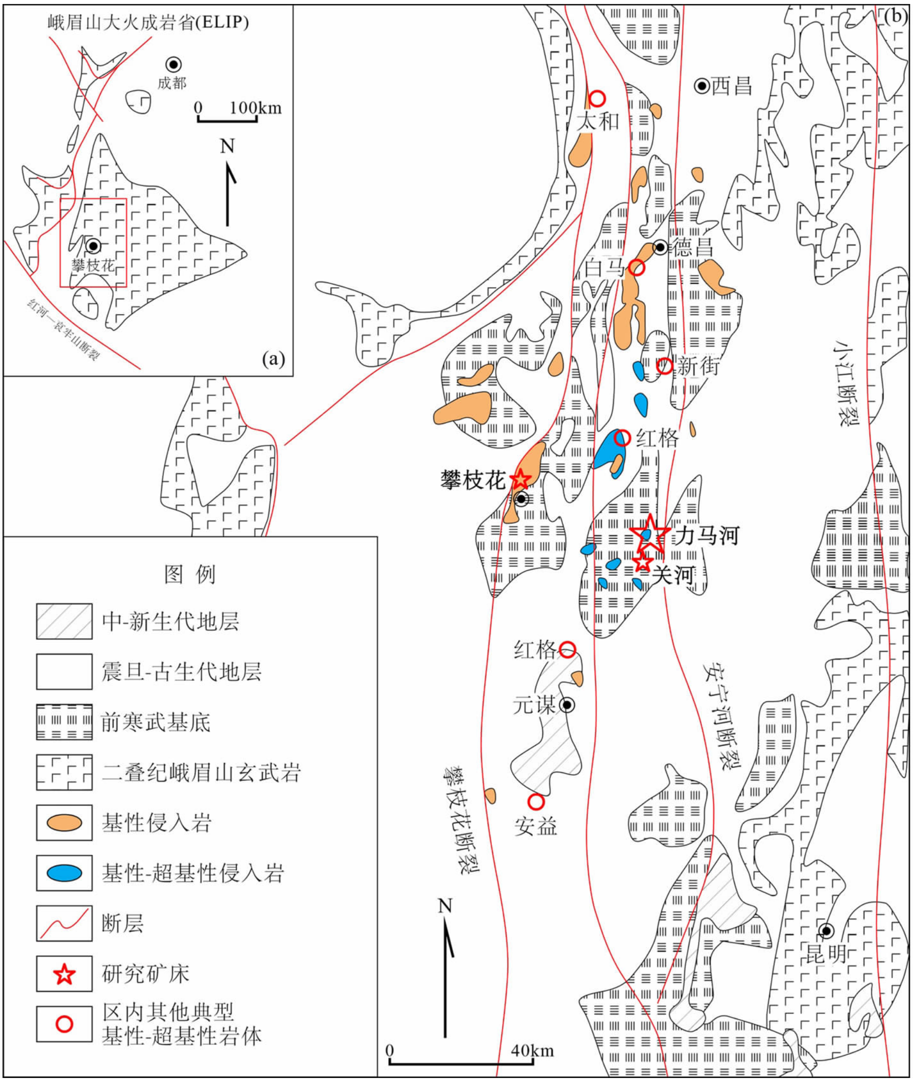

图 1 攀西地区位置图(a)及其区域地质简图(b，据郭艳峰等，2025)

Fig. 1 Location (a) and simplified regional geological map (b, after Guo *et al.*, 2025) of the Panxi region

入体就位于前寒武纪康定群、盐边群及会理群基底岩系内，其规模相差极为悬殊，主体为小型岩体，多呈岩盆、岩枝、岩株和脉状产出(党永西，2018)。研究区内，加里东-海西-印支期为岩浆活动的主体期。加里东期，安宁河地体与盐边地体的北向运移引起南北向挤压，从而诱发不同地区地幔发生深度不等的部分熔融，从而产生与钒钛磁铁矿矿床及岩浆铜镍硫化物矿床具有成因联系的镁铁质-超镁铁质岩体(党永西，2018)，海西期峨眉地幔柱的上涌作用导致扬子克拉通发生穹状隆升，并伴随大规模的玄武质岩浆喷溢(Xiao *et al.*, 2004；Xu *et al.*, 2001)。在康滇地轴、川滇台皱带及相邻造山带内，广泛发育二叠纪陆相与海相喷发的玄武岩(Zhang *et al.*, 2009)。依据 TiO_2 含量差异，可划分为高钛玄武岩与低钛玄武岩两类(Zhang *et al.*, 2009)。同期，镁铁质岩浆的侵入作用在康滇地轴及其邻区形成了大量镁铁质-超镁铁质岩体。岩浆活动在二叠系末期达到顶峰(宋谢炎等，2001；Zhang *et al.*, 2006)，安宁河与盐边地体于印支末期完成拼合，意味着该期岩浆活动就此终止(宋谢炎等，2001；Zhang *et al.*, 2006)。同期强烈的地幔柱活动则指示了深部富集地幔的形成(Chung and Jahn, 1995；Zhu *et al.*, 2003；Shellnutt *et al.*, 2020)。攀西地区 Cu-Ni(PGE)矿化岩体与峨眉山地幔柱活动产生的镁铁质-超镁铁质侵入体在空间上紧密共生，主体赋存于峨眉山玄武岩西区，经强烈抬升剥蚀而出露(Xu *et al.*, 2001, 2004)。受地幔柱与裂谷耦合作用制约，成矿岩体沿川滇构造带呈南北向线状展布，自北向南依次涵盖丹巴地区、大理-丽江地区及金平地区。典型的含矿岩体及矿床主要有柳坪 Cu-Ni-PGE 矿床、力马河 Cu-Ni 矿床、关河 Cu-Ni 矿床、白马寨 Cu-Ni 矿床以及金宝山贫硫化物 PGE 矿床(Zhou *et al.*, 2005；陶琰等，2007, 2008；Song *et al.*, 2008；Pang *et al.*, 2010)。

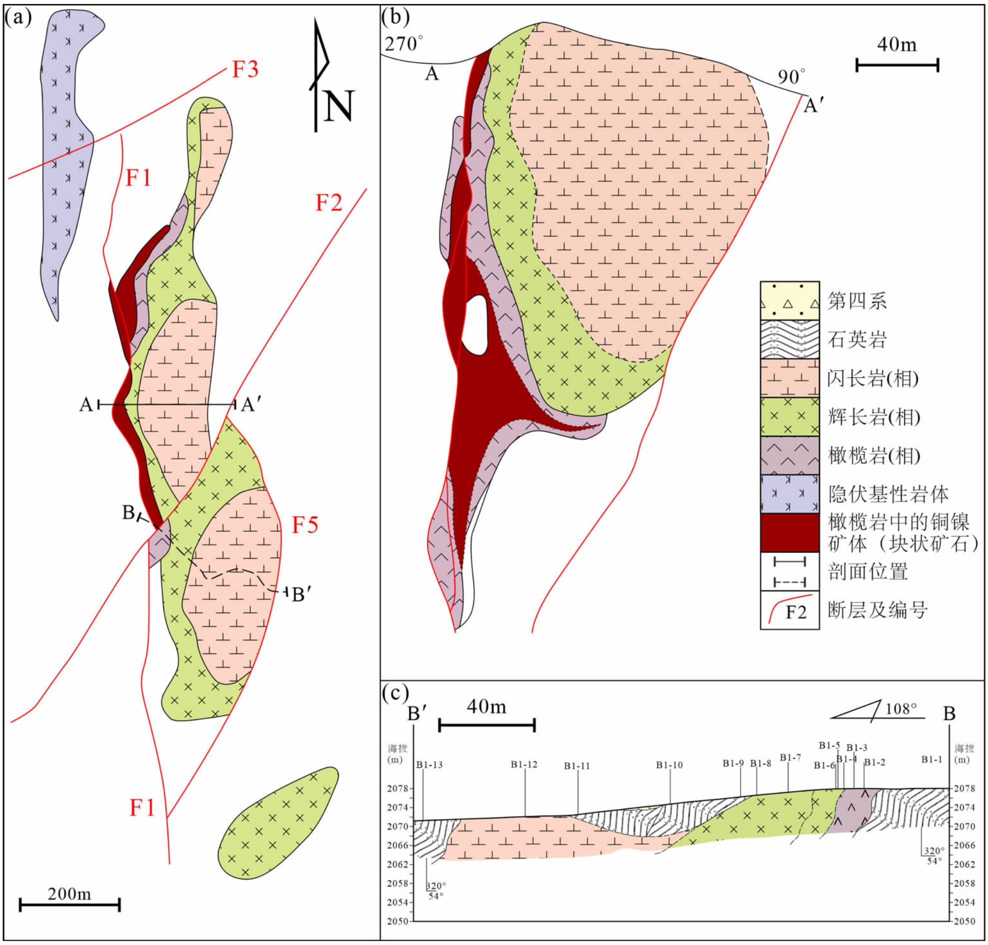

图 2 力马河矿床平面地质图(a, 据桂林冶金地质研究所等, 1974 修改)、剖面地质图(b, 据桂林冶金地质研究所等, 1974 修改)及实测剖面图(c)

Fig. 2 Geological map (a, modified after Institute of Metallurgical Geology, Guilin, *et al.*, 1974), geological cross-section (b, modified after Institute of Metallurgical Geology, Guilin *et al.*, 1974) and measured geological section (c) of the Limahe deposit

2 矿床地质特征

力马河铜镍硫化物矿床位于康滇地轴中段安宁河深断裂带东侧,受南北向主断裂控制,叠加康藏“歹”字型与新华夏系(陶琰等, 2008; 李莹, 2010),力马河矿床原勘探储量有镍品位 1.11 的矿石量 2.49×10^6t(陶琰等, 2008)。矿区力马河岩体沿南北向 F1 断裂不整合侵入力马河组(P_tl)与凤山营组(P_tf)接触界面(冉凤琴等, 2015),岩体南北向延展约 900m,东西向宽 120 ~ 140m(局部拓宽至 180m),平面形态为典型透镜状,剖面呈椭圆状。钻探资料证实其垂向延伸达 200 ~ 500m。区内一条南北向走滑断层将岩体错断为两段:北段为单斜构造,产状西倾;南段发育盆状向形(图 2a)。该侵入体的空间就位受基底断裂与围岩界面的共同制约。

含矿岩体分两阶段侵入:第一阶段辉长-闪长岩体受 F1 断裂控制,呈盆状单斜构造,由辉长岩相与闪长岩相渐变组成;第二阶段含矿超镁铁质岩脉(易剥橄榄岩与辉石橄榄岩渐变体)沿 F2 断裂贯入,形成陡倾(75° ~ 90°)透镜状岩脉群,具中部中粗粒易剥橄榄岩相-边缘中细粒辉石橄榄岩相分带,与辉长岩体具清晰侵入界面(图 2b)。矿体垂向分带显著:岩浆熔离-贯入-热液叠加成矿序列由下部浸染状-海绵陨铁状全岩矿化(橄榄岩相为主)、中部致密块状硫化物(>90% 硫化物)、上部斑杂状交代矿体构成。矿石矿物以黄铁矿、黄铜矿、磁黄铁矿、镍黄铁矿为主,发育典型海绵陨铁状矿石及块状矿石,赋存于超镁铁质岩脉内,受 F3 断裂控制的层间滑脱断层与 F1 断裂交汇部位主导定位。围岩蚀变具分带性:自矿体向外依次发育透闪石-绿泥石带、蛇纹石-滑石带、碳酸盐化带(李佑国, 2007; 汤中立等, 2011; Zhou *et al.*, 2008)。构造系统表现为:F1 断裂作为主导构造控制深位岩浆侵位;F2 继承性断裂主导含矿岩脉贯入;F3 叠接断裂系统(北东向张裂隙 + 北西向剪裂隙),形成矿体控制组合。

力马河岩体岩相分为闪长岩相-辉长岩相-橄榄岩相,其中橄榄岩相岩石类型包括二辉橄榄岩(橄榄石-单斜/斜方辉

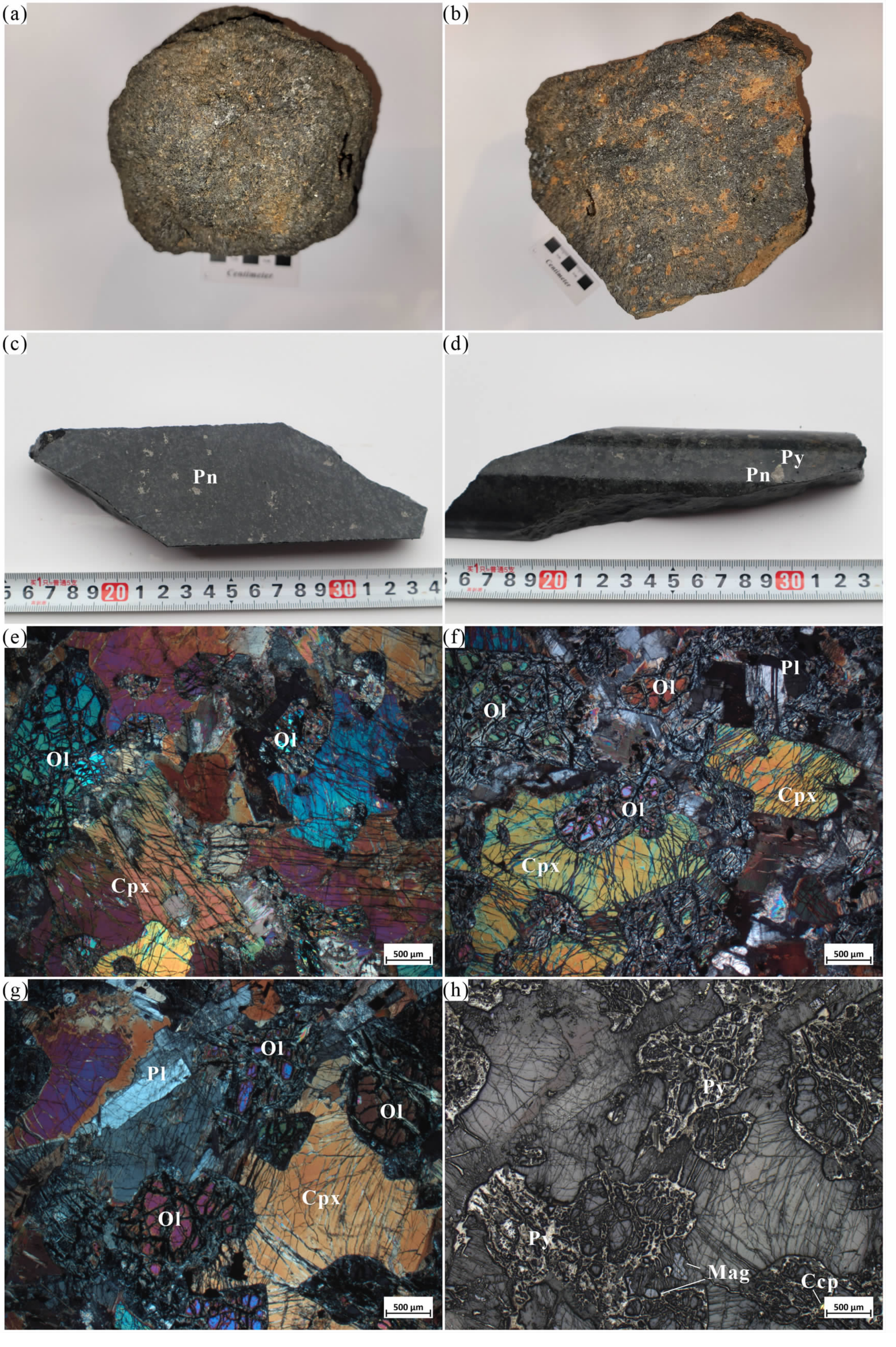

图 3　力马河矿床超镁铁质岩手标本与显微照片

(a)二辉橄榄岩手标本特征；(b)异剥橄榄岩手标本特征；(c-d)含矿二辉橄榄岩手标本特征；(e)二辉橄榄岩镜下矿物组合；(f)二辉橄榄岩镜下矿物组合；(g-h)异剥橄榄岩镜下矿物组合，黄铁矿以填隙形式分布于橄榄石颗粒之间．Ccp-黄铜矿；Cpx-单斜辉石；Mag-磁铁矿；Ol-橄榄石；

Pn-镍黄铁矿;Pl-斜长石;Py-黄铁矿

Fig. 3 Hand specimens and photomicrographs of ultramafic rocks from the Limahe deposit

(a) Hand specimen of lherzolite; (b) Hand specimen of wehrlite; (c-d) Hand specimen features of mineralized lherzolite; (e) Mineral assemblage of harzburgite under microscope; (f) Mineral assemblage of lherzolite under microscope; (g-h) Mineral assemblage of wehrlite under microscope, with pyrite occurring interstitially between olivine grains. Ccp-chalcopyrite; Cpx-clinopyroxene; Mag-magnetite; Ol-olivine; Pn-pentlandite; Pl-plagioclase; Py-pyrite

石组合)(图3a, c, e)、异剥橄榄岩(橄榄石-单斜辉石-黑云母组合)(图3b, g, h)及含长辉石橄榄岩(图3d)、橄榄辉石岩等,与邻区关河(橄榄岩-橄辉岩-辉长岩组合)和攀西南段白马寨(橄榄岩-斜方辉石岩-二辉岩组合)镍矿相关岩体相比,力马河岩体以镁铁-超镁铁质岩石发育齐全、分异演化充分、硫化物富集程度高为特点,反映克拉通边缘地幔柱作用背景下幔源岩浆多阶段分异-构造驱动贯入的成矿特征。其中力马河二辉橄榄岩呈黑色,主要矿物为橄榄石、单斜辉石与斜方辉石,次要矿物包括棕色角闪石和斜长石;金属矿物以镍黄铁矿、磁黄铁矿及黄铁矿为主;异剥橄榄岩呈黑色,具半自形中细粒粒状结构,主要矿物为橄榄石与单斜辉石,次要矿物含黑云母、棕色角闪石及斜长石,金属矿物为镍黄铁矿、磁黄铁矿与黄铁矿,常见橄榄石被包裹于单斜辉石之中,形成包含结构,指示橄榄石结晶早于单斜辉石。

3 样品采集和实验方法

本次采集了力马河矿床实测地质剖面及新施工的钻孔岩矿石样品,并采集攀西地区关河和白马寨岩矿石样品用于对比。其中力马河分析样品采集自实测勘探线西侧镁铁岩相带内(图2c),包括二辉橄榄岩、异剥橄榄岩、含长石辉石橄榄岩等;在关河矿床内采集了二辉橄榄岩样品;于白马寨矿床采集了辉石岩样品。样品制备探针片后,经系统显微镜下观察和分析,橄榄石与辉石用于电子探针测试并对同一样品同颗橄榄石与辉石进行LA-ICP-MS测试。

电子探针分析在中国地质科学院矿产资源研究所电子探针实验室进行,使用仪器为JXA-8230电子探针仪,设置加速电压为15kV,电流为20nA,束斑直径为1μm,仪器的检测限制为0.01% ~0.05%。采用ZAF校正法。

橄榄石、辉石原位微量元素分析在国家地质实验测试中心完成,使用仪器为Agilent 8900串联四极杆ICP-MS(ICP-MS/MS),配合激光剥蚀系统为NWR193。实验采用He作为剥蚀物质的载气,激光束斑直径为40μm、剥蚀时间为40s、脉冲频率6Hz、能量密度3J/cm^2,微量元素处理过程选用610作为外标。

4 测试结果

4.1 橄榄石成分特征

力马河岩体二辉橄榄岩中SiO_2含量38.49% ~54.90%,MgO含量17.45% ~43.07%,FeO含量4.87% ~18.39%,MnO含量0.05% ~0.27%,NiO含量0.03% ~0.17%;异剥橄榄岩中SiO_2含量36.27% ~39.27%,MgO含量40.82% ~44.73%,FeO含量16.62% ~19.71%,MnO含量0.18% ~0.28%,NiO含量0.01% ~0.25%;含长辉石橄榄岩中SiO_2含量38.35 % ~39.69%,MgO含量42.90% ~44.66%,FeO含量15.68% ~17.12%,MnO含量0.16% ~0.21%,NiO含量0.14% ~0.22%(附表1)。整体上看,力马河岩体Fo值介于0.78 ~0.91,主要落入贵橄榄石范畴,且异剥橄榄岩Fo值相对略低,Fo值的范围大,表示岩浆体系中橄榄石结晶的时间长。NiO含量0.06% ~0.22%、MnO含量0.05% ~0.28%与Fo值呈负相关演化趋势(图4),反映橄榄石结晶过程中Ni优先进入早期晶体,而Mn在残余熔体相对富集。CaO含量整体显著低于地幔橄榄石均值(0.4% ~0.6%)。

关河岩体二辉橄榄岩橄榄石SiO_2含量35.59% ~39.61%,MgO含量37.31% ~42.05%,FeO含量18.14% ~24.61%,MnO含量0.11% ~0.29%,NiO含量0.02% ~0.10%;辉石橄榄岩中SiO_2含量38.56% ~39.74%,MgO含量39.34% ~41.98%,FeO含量17.67% ~19.41%,MnO含量0.20% ~0.29%,NiO含量0.06% ~0.12%。整体上看,关河岩体Fo值介于0.73 ~0.81,全部落入贵橄榄石范畴,整体低于力马河。NiO含量(0.02% ~0.12%)、MnO含量(0.11% ~0.29%)与Fo值演化趋势与力马河相似,均为负相关,但NiO含量较力马河明显贫化(图4),这与晶体-熔体分配系数差异所决定的元素分馏规律相吻合:岩浆结晶过程中,橄榄石的元素含量变化受控于晶体-熔体间元素分配系数的差异:Ni为相容元素,优先进入橄榄石晶格,随着熔体演化与Fo值降低,残余熔体中Ni逐渐亏损,导致晚期结晶的橄榄石Ni含量降低;Mn为中等不相容元素,在熔体中相对富集,因此与Fo值呈负相关。

在橄榄石原始地幔标准化微量元素图解中(图5a;详细数据见附表2),力马河、关河、白马寨岩体橄榄石均具有相似的微量元素配分模式,除了2个力马河橄榄二辉岩样品具有明显的Ta负异常外,其余样品均具有明显的Ta、Pb、Sm正异常和Zr、Hf、Nb负异常。橄榄石球粒陨石标准化稀土元素图解中,关河部分样品呈现明显的Eu负异常,其中1件二辉橄榄岩橄榄石样品呈现明显的轻稀土亏损,重稀土富集的左倾型特征。力马河样品整体曲线较为平行一致,曲线呈轻稀土富集右倾型(图5b)。

图6表明,力马河岩体橄榄石的Cu、V、Sc、Ti含量分布

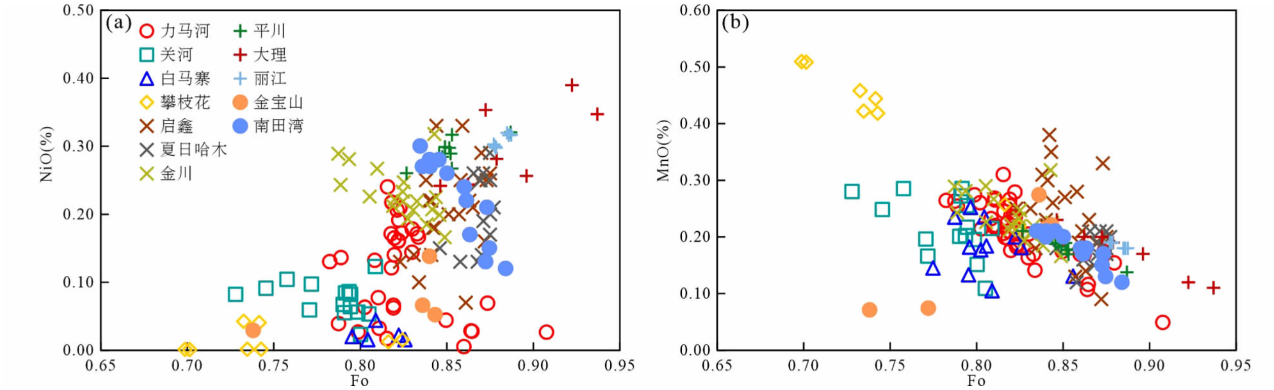

图 4 橄榄石 Fo 与 NiO(a)、MnO(b)元素含量二元相关图

攀枝花数据引自高文元，2018；启鑫数据引自庞振阵等，2024；夏日哈木数据引自李中州等，2023；金川数据引自彭璐，2023；平川数据引自张磊等，2022；大理-丽江数据引自蔡文昌，2021；金宝山数据引自王良果，2015；南田湾数据引自 Zhang *et al.*，2017. 后图引用数据来源同此图

Fig. 4 Binary correlation diagram of Fo versus NiO (a) and MnO (b) contents in olivine

Data sources: Panzhihua from Gao, 2018; Qixin from Pang *et al.*, 2024; Xiarihamu from Li *et al.*, 2023; Jinchuan from Peng, 2023; Pingchuan from Zhang *et al.*, 2022; Dali-Lijiang from Cai, 2021; Jinbaoshan from Wang, 2015; Nantianwan from Zhang *et al.*, 2017. The data source cited for the subsequent figure is identical to that for this figure

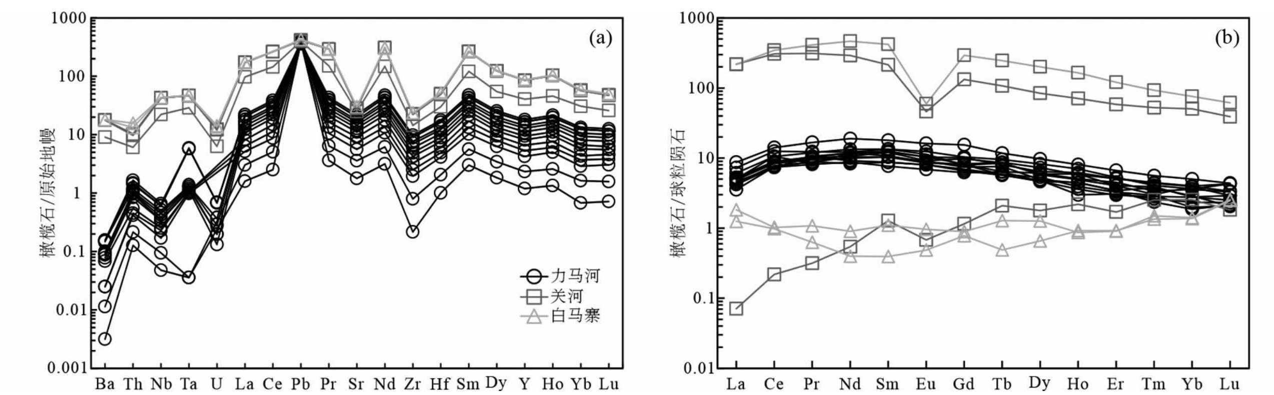

图 5 力马河、关河、白马寨岩体橄榄石原始地幔标准化微量元素蛛网图(a)和球粒陨石标准化稀土元素配分图(b)(标准化值据 Sun and McDonough, 1989)

Fig. 5 Primitive mantle-normalized trace element spider diagrams (a) and chondrite-normalized rare earth element patterns (b) of olivine from the Limahe, Guanhe, and Baimazhai intrusions (normalization values after Sun and McDonough, 1989)

集中，变化幅度有限；白马寨岩体 Cu 含量较低，V、Sc 含量较高；关河岩体 Cu、Sc 含量较低，Cu、V、Sc、Ti 的含量分布较为分散，变化区间较大；攀枝花岩体的 Cu、V、Sc 含量最低。

4.2 辉石成分特征

力马河单斜辉石展现出典型镁铁质岩浆结晶序列特征，其 SiO_2(41.08% ~ 53.25%)与 MgO(14.34% ~ 27.72%)含量指示以普通辉石-透辉石为主(图 7、附表 3)，$Mg^{\#}$(73.42 ~ 87.51)集中分布于镁质辉石范围，指示母岩浆具较高的镁铁比。CaO(11.36% ~ 21.01%)与 Al_2O_3(1.26% ~ 12.81%)的显著富集暗示其形成于相对高压条件。$Mg^{\#}$-氧化物协变图解(图 8)显示，Al_2O_3 与 $Mg^{\#}$ 呈负相关，这与岩浆分异过程中 Al 优先进入熔体相的行为一致，负相关性较关河更显著，暗示更强的分离结晶作用。TiO_2(0.43% ~ 4.61%)与 Na_2O(0.16% ~ 1.75%)呈显著正相关，可能反映晚期熔体中碱性组分富集。

在单斜辉石原始地幔标准化微量元素图解中(图 9a；详细数据见附表 4)，3 个矿区辉石均具有相似的微量元素配分模式，所有样品均具有明显的 Nb、Ta、Nd、Sm 正异常和 Th、U、Sr、Zr 负异常。辉石球粒陨石标准化稀土元素图解中，关河部分样品呈现明显的 Eu 负异常，白马寨样品呈现 Sm、Gd、Ho 负异常，力马河样品地球化学行为较为一致，曲线呈轻稀土富集右倾型(图 9b)。

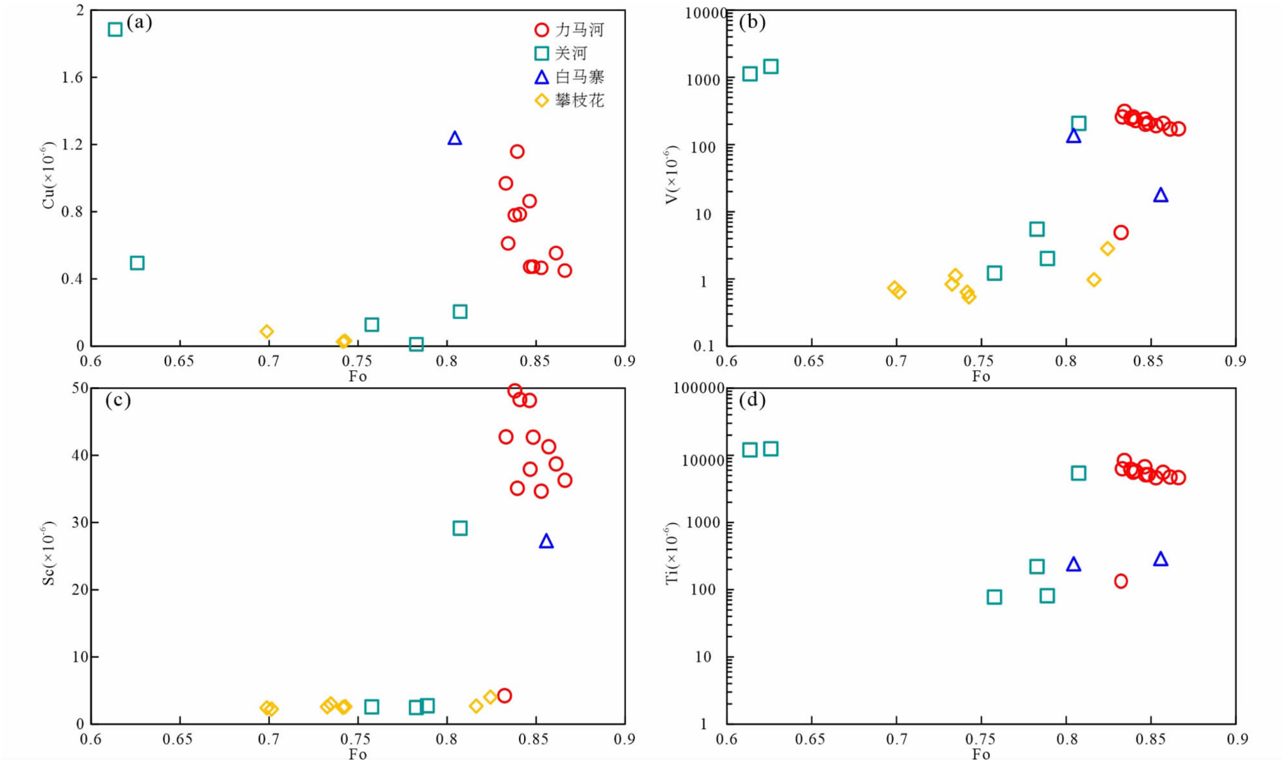

图 6 橄榄石 Fo 与 Cu(a)、V(b)、Sc(c)和 Ti(d)元素含量二元相关图

Fig. 6 Binary correlation diagram of Fo versus Cu (a), V (b), Sc (c) and Ti (d) contents in olivine

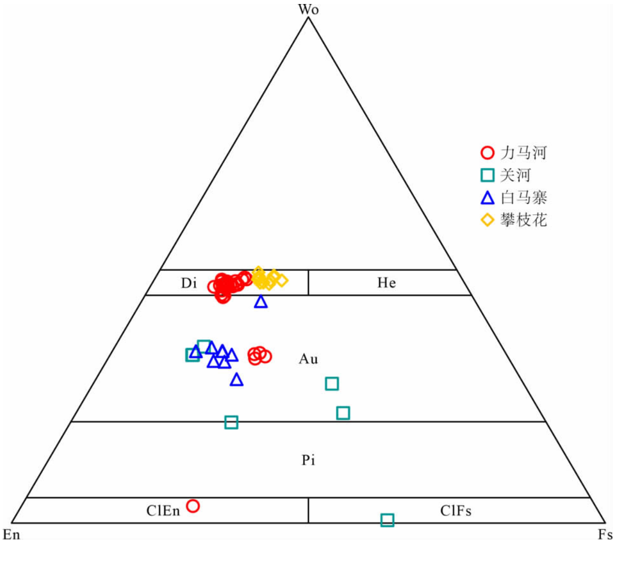

图 7 辉石 Wo-En-Fs 图解(据 Morimoto *et al.*, 1988)

攀枝花数据引自高文元, 2018,后图引用数据来源同此图. Di-透辉石;He-钙铁辉石;Au-普通辉石;Pi-易变辉石;ClEn-斜顽辉石;ClFs-斜铁辉石

Fig. 7 Wo-En-Fs diagram of pyroxene (after Morimoto *et al.*, 1988)

Data source: Panzhihua from Gao, 2018. The data source cited for the subsequent figure is identical to that for this figure. Di-diopside; He-hedenbergite; Au-augite; Pi-pigeonite; ClEn-clinoenstatite; ClFs-clinoferrosilite

5 讨论

5.1 岩浆源区特征与成分

5.1.1 岩浆源区性质

橄榄石作为幔源岩浆早期演化阶段的结晶矿物,其微量元素成分及比值是判别地幔源区特征的关键地球化学指标(Sobolev *et al.*, 2005, 2007; Lee *et al.*, 2010; Søager *et al.*, 2015; Ren *et al.*, 2017; Yao *et al.*, 2019; Xu *et al.*, 2020; Mao *et al.*, 2022)。橄榄岩部分熔融形成的橄榄石通常具有高 Mn/Zn(>15)和低 10000×Zn/Fe(<11)(Lee *et al.*, 2010; Howarth and Harris, 2017; Marschall *et al.*, 2017; Jeffcoate *et al.*, 2007)的特征,而源自辉石岩地幔的橄榄石则表现相反,这一差异可有效示踪源区性质与熔融过程(图 10)。橄榄石的 V/Sc 比值、Fo 值及 Ni、Li 含量特征可进一步指示不同岩浆源区物理化学条件的差异(图 11)。

力马河二辉橄榄岩、异剥橄榄岩的橄榄石显示高 V/Sc 比值、高 Fo 值、低 Li、低 Mn 含量(图 11),反映其母岩浆源自深部石榴子石的还原性橄榄岩地幔特征,力马河岩体橄榄石中 V 含量明显偏高。V 属于变价元素,其在橄榄石与熔体间的分配系数随氧逸度增高而递减,由此推断该岩体成矿岩浆的氧逸度可能低于其他矿区,环境更为还原(图 6),高 V/Sc 比值指示岩浆形成于低氧逸度环境(图 11)。邻区关河岩体

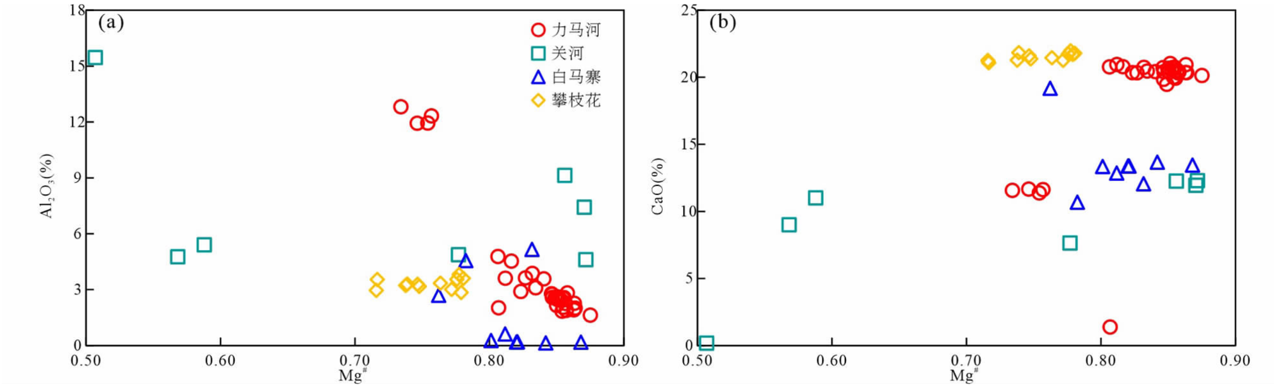

图 8 辉石 $Mg^{\#}$与氧化物图解

Fig. 8 Diagrams of pyroxene $Mg^{\#}$ versus oxides

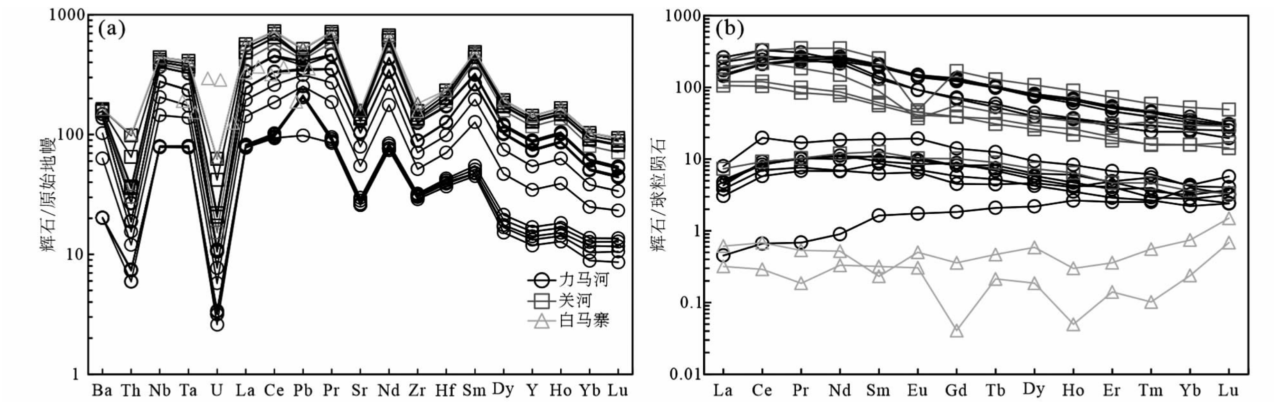

图 9 力马河、关河、白马寨岩体单斜辉石原始地幔标准化微量元素蛛网图(a)和球粒陨石标准化稀土元素配分图(b)(标准化值据 Sun and McDonough, 1989)

Fig. 9 Primitive mantle-normalized trace element spider diagrams (a) and chondrite-normalized rare earth element patterns (b) of clinopyroxene from the Limahe, Guanhe, and Baimazhai intrusions (normalization values after Sun and McDonough, 1989)

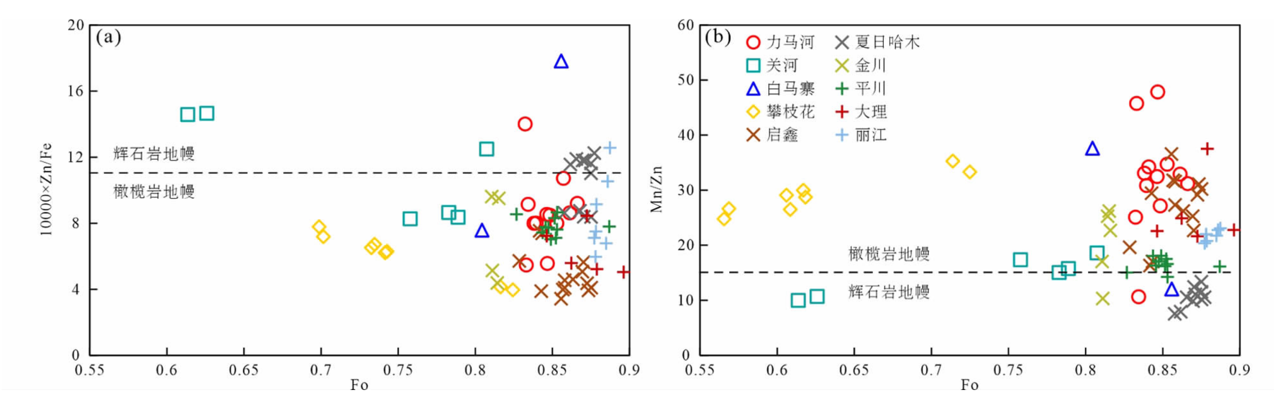

图 10 橄榄石 Fo 与 10000 × Zn/Fe(a)、Mn/Zn(b)相关图

Fig. 10 Binary correlation diagrams of Fo versus 10000 × Zn/Fe (a) and Mn/Zn (b) in olivine

也表现为类似的地球化学特征，但其稀土元素图解中(图5b)指示其岩浆源区可能来自于部分熔融后的亏损地幔。力马河与关河的矿物化学成分数据判断源区性质与前人利用全岩微量元素与稀土元素数据得出的结论相对应(王萌等, 2011; 朱飞霖等, 2017)。相比之下，攀枝花岩体橄榄石呈现低 V/Sc 比值、较低 Fo 值、及贫 Li、高 Mn 含量(图 11)，表明

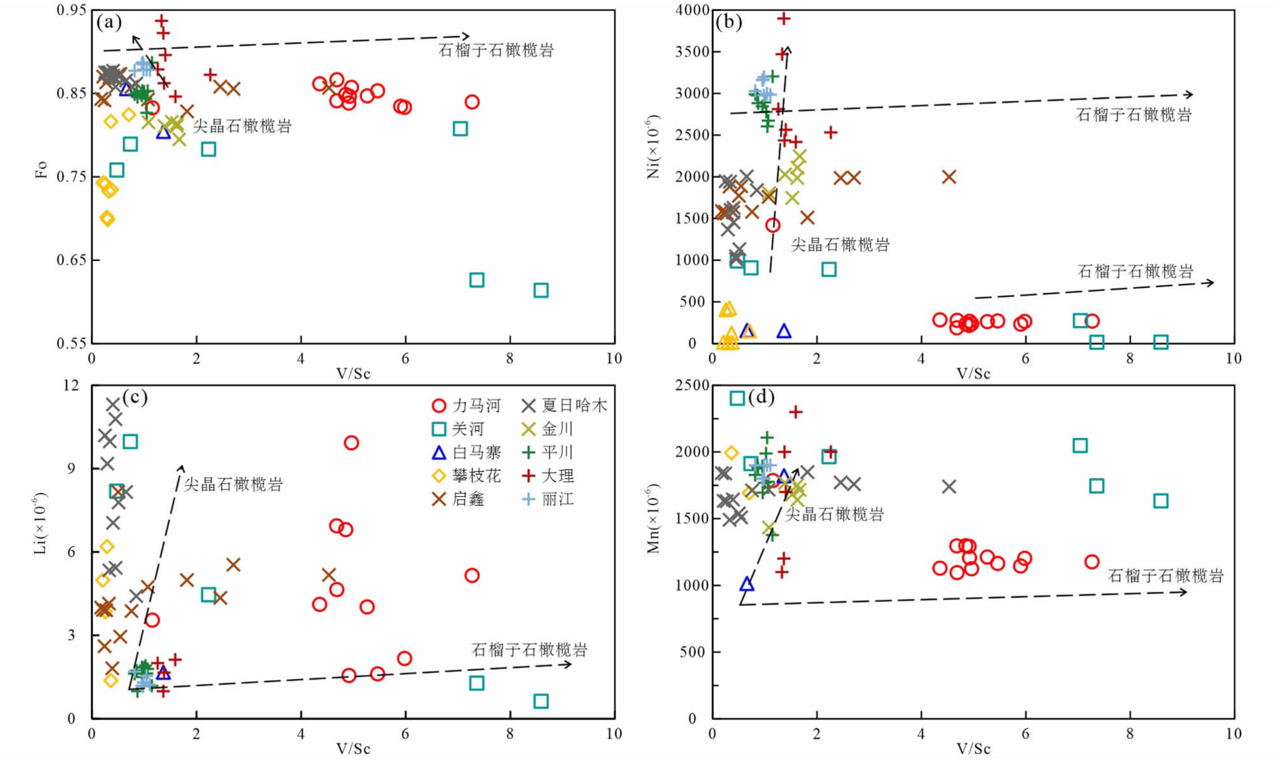

图 11 橄榄石 V/Sc 与 Fo(a)、Ni(b)、Li(c)、Mn(d)相关图(底图据毛亚晶等, 2024 修改)

Fig. 11 Binary correlation plots of V/Sc vs. Fo (a), Ni (b), Li (c), and Mn (d) in olivine (base map modified after Mao *et al.*, 2024)

其母岩浆起源于浅部尖晶石橄榄岩地幔,但前人全岩分析结果(赵瑛, 2020)及同位素特征(艾羽等, 2006)表明攀枝花岩体源自与峨眉山高 Ti 玄武岩相同的石榴子石地幔。橄榄石的地球化学特征记录了岩浆从源区分离后、最终侵位前的演化历史,而全岩 Sr-Nd-Pb 同位素则提供了约束其地幔源区性质的可靠依据,其微量元素比值出现的高 Mn,高 Li 异常以及低 V/Sc 比值应该是源区受到岩石圈地幔混染的结果(见后文)。平川苦橄岩、大理苦橄岩、丽江苦橄岩的橄榄石成分趋势与石榴子石地幔橄榄岩一致,这一结论与前人的全岩数据资料呈现出高度的可比性(柏中杰等, 2019; 罗阳阳, 2025)。夏日哈木岩体橄榄石 Mn/Zn、10000Zn/Fe 比值表现为辉石岩地幔源区的地球化学特征(图 10),但其 V/Sc 比值与 Ni、Li、Mn 含量关系表明其也受到尖晶石橄榄岩地幔的影响(图 11)。结合前人基于全岩样品获得的分析数据表明(张志炳等, 2016),夏日哈木岩体地幔源区为亏损的软流圈尖晶石二辉橄榄岩,源区有辉石岩地幔物质加入。金川岩体,启鑫岩体橄榄石部分展现出石榴子石橄榄岩源区特征,还有部分表现为尖晶石橄榄岩源区特征,但其整体趋势说明金川、启鑫岩体母岩浆表现出与尖晶石橄榄岩地幔源区的高度一致性(图 11),这一结论也得到了前人全岩分析结果及同位素特征(Lu *et al.*, 2019; 徐文博, 2023)的佐证。此外, Li 含量偏高可能是深部地幔交代流体参与的结果。

两类成矿(铜镍硫化物矿床与钒钛磁铁矿矿床)岩体的地球化学分异揭示了地幔源区垂向非均质性对成矿潜力的控制:深部还原性石榴子石地幔(>75km)源于地幔柱边缘的高程度熔融,其源区为 OIB 型富集橄榄岩地幔,地壳混染微弱,地球化学属性与洋岛玄武岩类似(Zhou *et al.*, 2008; Shellnutt *et al.*, 2009)。此类岩浆富 Fe-Ti 而贫挥发分,上升过程中主要经历氧化物分离结晶,因而形成以 Fe-Ti 氧化物堆晶为主的钒钛磁铁矿矿化类型(攀枝花型),其伴生 Ni-Cu-PGE 矿化潜力有限(Lu *et al.*, 2019);浅部氧化性尖晶石地幔(<60km)或尖晶石-石榴子石过渡带地幔在板块边缘伸展背景下往往叠加了俯冲物质的交代作用(Foley *et al.*, 2013),形成辉石岩-橄榄岩混合源区(Song *et al.*, 2016)。此类源区部分熔融产生的母岩浆具有高氧逸度、富 Ni-Co-Cu、贫 PGE 的特征,其硫化物饱和常由地壳 S 的加入触发,有利于 Ni-Cu 硫化物富集(金川、启鑫、夏日哈木型),并可形成伴生 Co 的 Ni-Cu 矿化,但 PGE 富集程度有限。

地幔岩浆向地壳的运移通常可视为近绝热快速过程,硫化物饱和的主控因素为压力,其原因在于硫在岩浆中的溶解度与压力呈负相关(Mavrogenes and O'Neill, 1999),若无硫、流体或同化混染等外来物质的补充,岩浆在上升减压过程中难以自发达到硫化物饱和,因而无法形成大型铜镍硫化物矿床(Naldrett, 2004, 2010)。力马河镁铁-超镁铁质岩体的橄

榄石(二辉橄榄岩、异剥橄榄岩)指示其母岩浆源自深部还原性石榴子石地幔，尽管尖晶石橄榄岩地幔更有利于 Ni-Cu 硫化物富集，但氧逸度的改变在结晶分异过程中并不能显著降低硫的溶解度(Chin *et al.*, 2014)，力马河岩体的源区属性有别于典型 Ni-Cu 成矿岩体，但其仍形成了具有经济效益的铜镍硫化物矿床。这一事实意味着，在岩浆演化过程中必然存在促使硫化物提前饱和的特殊过程，其中地壳混染是最可能的诱因。下文的岩石化学与矿物化学证据将为这一推论提供关键支撑，这也解释了其源区属性虽与典型 Ni-Cu 成矿源区不同但仍形成铜镍硫化物矿床的根本原因。

5.1.2 *母岩浆成分*

超镁铁岩浆初始阶段，橄榄石与熔体之间的 Fe-Mg 分配系数($K_D = X^{Ol}_{(FeO/MgO)}/X^{melt}_{(FeO/MgO)}$)不随岩浆结晶分异过程的进行而改变，通常稳定于 0.3～0.34 范围内(Barnes *et al.*, 2013)。由此，可以根据与熔体平衡结晶的橄榄石 Fo 值(Fo $= X^{Ol}_{Mg}/(X^{Ol}_{Fe} + X^{Ol}_{Mg})$)获得母岩浆的 MgO/FeO 比值。进一步的，根据质量平衡原理及相平衡关系公式(Li and Ripley, 2011)：

$$W_{MgO}/W_{FeO} = 0.56095 \times K_D \times Fo/(1 - Fo)$$

$$Mg^{\#} = X^{Melt}_{Mg}/(X^{Melt}_{Fe} + X^{Melt}_{Mg}) = 1/(1 + (1 - Fo)/(K_D \times Fo))$$

$$W_{MgO} = 0.56095Kd \times Fo/(1 - Fo)W^{T}_{FeO}$$

基于橄榄石矿物化学与全岩组成，可以估算出镁铁-超镁铁质岩体的原始岩浆成分(Chai and Naldrett, 1992)。本文获得力马河二辉橄榄岩中橄榄石 Fo 值最大为 90.77，判断为母岩浆初始阶段结晶产物，橄榄石与熔体之间的 Fe-Mg 分配系数按 0.3(Roeder and Emslie, 1970)。计算得出力马河岩体的母岩浆成分：超镁铁质岩体母岩浆 MgO 含量约 12.0%，FeO^T 的含量约 8.7%，属高镁玄武质岩浆。镁铁质岩体母岩浆 MgO 含量约 8.2%，FeO^T 的含量约 10.6%，属拉斑玄武岩质岩浆(岩石化学数据引自陶琰等, 2008；李莹, 2010)，与峨眉山低 Ti 玄武岩具有密切的亲缘关系。年代学及地球化学对比表明，力马河岩体与杨柳坪、白马寨、朱布、金宝山等岩体同为峨眉山地幔柱的产物(陶琰等, 2007；尤敏鑫等, 2017)。值得注意的是，力马河岩体代表了母岩浆演化至晚期阶段的产物，这与金宝山、朱布等 PGE 矿床(早期演化阶段)形成鲜明对比，反映了同一地幔柱源区岩浆在不同演化阶段以及不同程度的地壳混染作用下的成矿分异(王焰, 2008；尤敏鑫等, 2017)。

峨眉山大火成岩省高低 Ti 玄武岩的分区特征深刻反映了地幔柱的垂向非均质性与侧向分带(Xu *et al.*, 2007)。这一分区不仅控制了岩浆的 Ti 含量，也深刻制约了成矿类型：高 Ti 岩浆趋向于形成 Fe-Ti 氧化物矿床(攀枝花型)，低 Ti 岩浆则更有利于 Ni-Cu 硫化物富集(力马河、白马寨型)(艾羽等, 2006；陶琰等, 2007, 2008；王焰, 2008)。

启鑫岩体为地幔柱-岩石圈相互作用产物，母岩浆源于岩石圈地幔部分熔融(Liu *et al.*, 2017；Xue *et al.*, 2019)；夏日哈木岩体属造山带伸展背景下(张志炳等, 2016)软流圈上涌形成的低 Ti、高 Mg 拉斑玄武质岩浆(Sun *et al.*, 1991；张照伟等, 2021)；金川岩体具大陆裂谷背景，母岩浆为高镁玄武岩浆(徐章华等, 1998)。三者均区别于峨眉山地幔柱直接起源的岩体。

上述岩体的母岩浆成分对比揭示了一个重要的成因规律：地幔源区的垂向非均质性与构造背景共同控制着岩浆成分与成矿专属性。力马河、白马寨等攀西地区岩体与峨眉山低 Ti 玄武岩同源，同为地幔柱边缘或晚期演化的产物；攀枝花则代表地幔柱的高 Ti 端元；启鑫岩体则为地幔柱-岩石圈相互作用的过渡类型。夏日哈木岩体与金川岩体虽具低 Ti、高 Mg 特征，但分属造山带伸展与大陆裂谷背景，表明地幔柱并非 Ni-Cu 硫化物成矿的唯一深部驱动机制，软流圈上涌、岩石圈伸展同样可以诱发地幔熔融并形成含矿岩浆。

力马河、关河、白马寨岩体的单斜辉石地球化学特征显示其具有亚碱性系列特征(图 12a)，攀枝花岩体的单斜辉石特征反应其属于亚碱性-碱性系列；在单斜辉石 SiO_2-Na_2O-TiO_2 三角图解中(图 12b)，4 个矿区的样品大部分位于拉斑玄武岩系列的范围内。在 2 个图解中，力马河的极少部分单斜辉石样品(寄主岩石为异剥橄榄岩)位于碱性-过碱性的范围内，异剥橄榄岩作为一种典型的堆晶岩，代表了岩浆演化至较高程度时的产物，其中的单斜辉石结晶于经历显著分离结晶作用后残余的熔体中。此时熔体已富集碱金属与铝等不相容元素，导致部分单斜辉石虽在化学成分上呈现出向碱性系列偏移的趋势，但其本质上仍是从亚碱性母岩浆演化而来的晚期堆晶矿物。力马河超镁铁质岩体单斜辉石的亚碱性特征证实了岩浆是在拉斑环境中结晶分异的；而高镁玄武质母岩浆揭示了其地幔柱来源的原始属性。两者共同印证了力马河岩体是峨眉山地幔柱产生的高镁拉斑玄武质岩浆经过长期演化、并在浅部地壳发生结晶分异的产物。

5.2 岩浆演化与镍成矿

5.2.1 *地壳混染作用*

幔源岩浆在向地壳浅部上升演化过程中达到硫饱和，是形成岩浆铜镍硫化物矿床的重要条件。作为诱发硫饱和的主导机制，地壳混染在幔源岩浆演化中也同样发挥着重要作用(Li *et al.*, 2013；Naldrett, 1989)。一方面壳源物质的加入可显著改变幔源岩浆的成分(DePaolo, 1981；Spera and Bohrson, 2001)；另一方面富硅或富硫物质的加入能分别通过降低硫溶解度或直接增加硫含量来使得岩浆中橄榄石与硫化物共结比例的急剧增大，引发硫化物熔离，进而驱动成矿作用(Arndt *et al.*, 2003)。岩浆演化过程中 Li 的富集是示踪陆壳物质加入的有效指标(Brenan *et al.*, 1998；Rudnick and Gao, 2003；Prelević *et al.*, 2013)，La/Nb 和 Zr/Hf 等元素比值受岩浆分离结晶作用影响较小，亦对壳源混染作用较为敏感(Baker *et al.*, 1997；Macdonald *et al.*, 2001)，可有效识别岩浆演化过程中的地壳混染作用。

橄榄石 Li 含量部分样品指示板内岩浆属性，与岩石圈

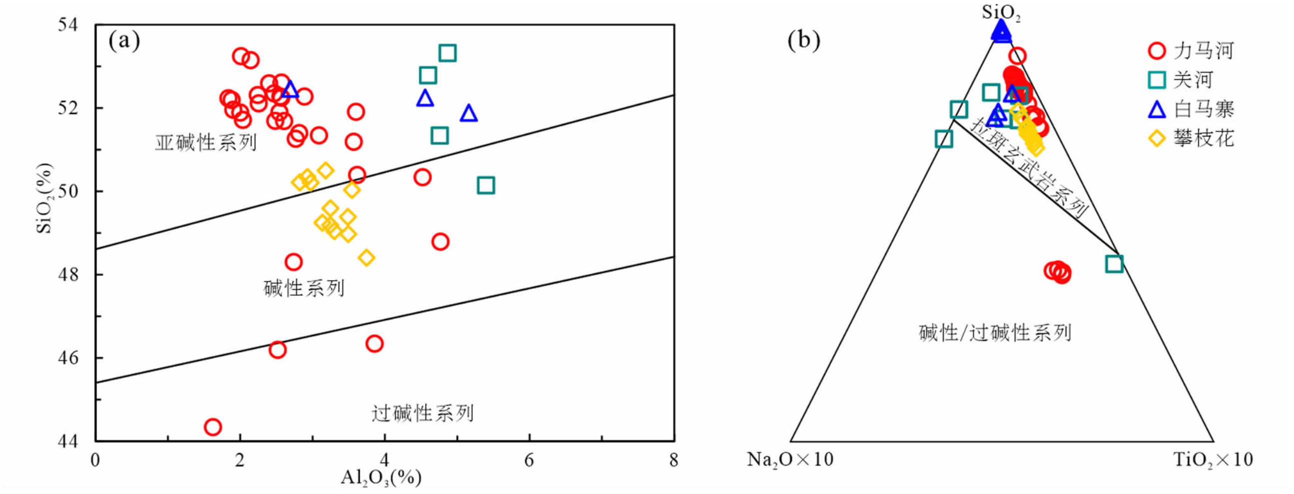

图 12 单斜辉石 Al_2O_3-SiO_2 图解(a)SiO_2-$Na_2O\times10$-$TiO_2\times10$ 三角图解(b)(底图据邱家骧和廖群安, 1996 修改)

Fig. 12 Al_2O_3 vs. SiO_2 plot (a) and SiO_2-($Na_2O\times10$)-($TiO_2\times10$) ternary diagram (b) for clinopyroxenes (base map after Qiu and Liao, 1996)

地幔和洋壳相比,陆壳及陆源沉积物更富集 Li (Foley *et al.*, 2013),因此陆壳物质经再循环加入地幔会提升地幔的 Li 丰度(Brenan *et al.*, 1998; Rudnick and Gao, 2003),部分异常高值则暗示岩浆源区存在流体交代地幔与壳源组分的叠加。力马河、白马寨镁铁-超镁铁岩体橄榄石(二辉橄榄岩、异剥橄榄岩)Li 含量表明岩浆演化过程中经历过显著的壳源组分混染;攀枝花岩体橄榄石表明其经历的混染有限(图 13f)。$(Th/Yb)_{PM}$-$(Nb/Th)_{PM}$图解中,力马河超镁铁质岩体(二辉橄榄岩、异剥橄榄岩)极低的$(Nb/Th)_{PM}$比值(0.06~0.77),接近上地壳线,指示强烈 Nb 负异常与地壳混染作用(Rollinson, 1993)。$(Th/Ta)_{PM}$-$(La/Nb)_{PM}$图解显示样品主要落入中-上地壳混染趋势带。力马河和白马寨作为攀西地区典型的成镍矿岩体,其超铁单元(含长辉石橄榄岩、易剥橄榄岩、橄榄辉石岩)的 Nb/Hf、Ce/Pb、Nd/U 比值显著偏离原始地幔、MORB 及 OIB 范围,趋近上地壳平均值,指示其母岩浆经历了明显的地壳物质同化混染作用。此外,力马河岩体的低 Ce/Pb 比值(0.87~11.69)显著低于幔源岩浆和平均陆壳,指示地幔源区遭受了源自板片的流体交代。综合地球化学指标表明,力马河岩体是交代地幔部分熔融的产物,并经历了显著的地壳物质混染。攀枝花岩体$(Th/Ta)_{PM}$-$(La/Nb)_{PM}$图解显示其受岩石圈地幔混染(图 13a),较高的 Nb/Th 和 La/Nb 比值、较低的 Th/Yb 和 La/Sm 比值(图 13b, e),说明岩体形成过程中并不存在强烈的陆壳混染,结合前人的 Sr-Nd-Pb 同位素数据(Zhang *et al.*, 2009),更加印证了地壳混染在攀枝花岩体成岩成矿过程中影响不大这一结论。启鑫岩体、夏日哈木岩体也体现出其岩浆源区具有地壳混染特征,二平川苦橄岩、大理苦橄岩以及丽江苦橄岩则基本落入板内岩浆岩范围内,少有壳源混染(图 13f)。总之,混染作用对于镍矿富集至关重要,其核心在于它能触发并促进岩浆中硫化物熔体的熔离,而镍元素具有强烈的亲硫性,会优先进入这些熔离出来的硫化物熔体中,从而实现富集形成矿床。

5.2.2 硫化物熔离作用

橄榄石中 Ni 含量受母岩浆成分及硫化物熔离的影响,可作为硫化物熔离作用的发生及强度的判别标志(Brenan and Caciagli, 2000)。早阶段橄榄石结晶与硫化物熔离造成残余硅酸盐熔体 Ni 亏损。橄榄石 Ni 含量及 Fo 值可有效指示岩浆演化过程中的硫饱和状态,硫化物熔离的发生将导致晶出橄榄石 Ni 含量降低,并使 Ni 与 Fo 值呈负相关关系(Naldrett, 1999)。

力马河岩体橄榄石的 NiO 含量介于 0.01% 至 0.25%,显著低于与地幔岩平衡的原始玄武岩浆中结晶的橄榄石(约 0.4%),显示强烈亏损 Ni。在 Fo-NiO 相关图解中,力马河超镁铁质岩体(二辉橄榄岩、异剥橄榄岩)矿物化学特征反映了硫化物已发生熔离(图 14b)。橄榄石 Ni 含量的变化同样明确指示了硫化物熔离与橄榄石结晶的时序关系:当硫化物熔离不晚于橄榄石分离结晶时,Ni 优先进入硫化物相,致使结晶橄榄石的 Ni 含量快速下降(图 14b 曲线 B);当硫化物发生熔离作用后,橄榄石随后与硫化物熔体发生再平衡,其 Ni 含量则会随着结晶作用的进行而呈现升高趋势(图 14b 曲线 A)。白马寨、南田湾岩体橄榄石 NiO 与 Fo 呈负相关,说明其母岩浆在早期发生了较多的硫化物熔离,这种趋势表明,硫化物熔离早于或同步于橄榄石的分离结晶,当硫化物先结晶时,Ni 优先进入硫化物相,导致后续橄榄石中 Ni 含量迅速降低形成富 Ni-Cu 岩浆。关河岩体橄榄石 NiO 与 Fo 呈正比,矿相学观察显示,硫化物主要分布于橄榄石和辉石粒间,且包含硫化物珠滴的橄榄石具有较低的 Fo 值,这种趋势指示硫化物熔离发生于母岩浆演化的晚期,矿相学观察显示,硫化物主要分布于橄榄石和辉石粒间,且包含硫化物珠滴的橄

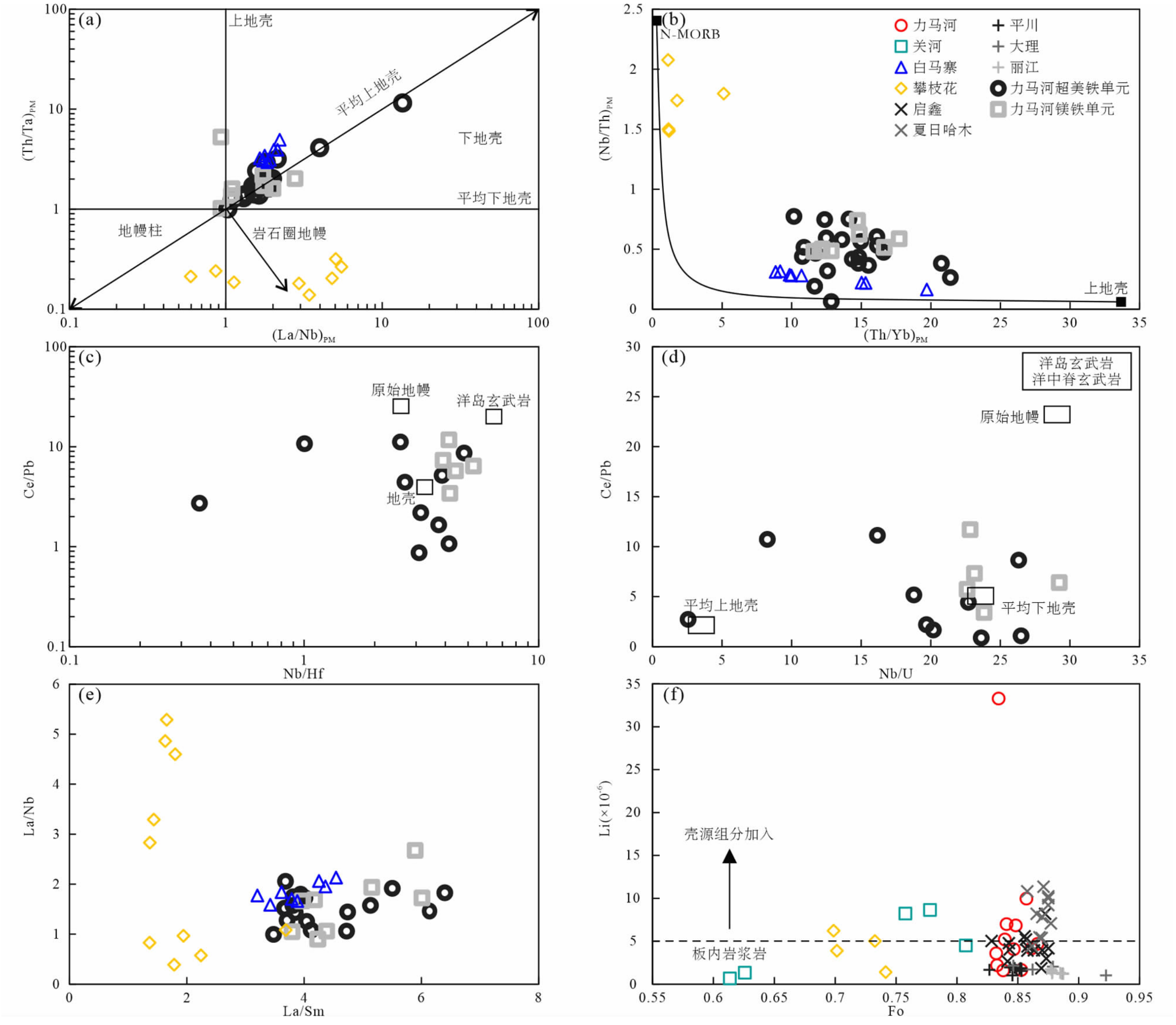

图 13 地幔源区判别图(a，底图据 Neal *et al.*，2002；b，底图据 Zhao *et al.*，2015)

力马河岩体全岩数据引自陶琰等，2008；李莹，2010；白马寨和攀枝花岩体全岩数据分别据管涛等，2006 和艾羽等，2006

Fig. 13 Discrimination diagrams for mantle source regions (a, base map after Neal *et al.*, 2002; b, base map after Zhao *et al.*, 2015)

Whole-rock data for Limahe intrusion from Tao *et al.*, 2008 and Li, 2010; for Baimazhai and Panzhihua intrusions from Guan *et al.*, 2006, and Ai *et al.*, 2006

榄石具有较低的 Fo 值，这表明橄榄石先结晶，随后粒间硫化物熔体与已结晶的橄榄石发生再平衡，导致 NiO 含量随着结晶进行呈现升高趋势，反映硫化物熔离发生于母岩浆演化晚期，从而导致仅形成低品位的岩浆硫化物矿化。攀枝花岩体橄榄石 NiO 随 Fo 增加基本不变，呈微弱增加趋势，攀枝花岩体经历了多次富 Fe-Ti 岩浆的补充(Haggerty，1991；钟祥，2019)，岩浆体系富集 Fe-Ti，Ni 的分配行为主要受控于硅酸盐矿物结晶，硫化物熔离作用不显著，因此橄榄石 Ni 含量未出现明显亏损，而是随岩浆分离结晶呈现微弱富集趋势。金川岩体橄榄石 NiO 随 Fo 增加而降低，指示硫化物熔离早于或同步于橄榄石结晶，有利于形成 Ni-Cu 硫化物矿床。夏日哈木岩体橄榄石的 NiO 与 Fo 呈正相关性，结合前人对其全岩的同位素研究(李文渊，2015)、尖晶石与斜方辉石的矿物学研究(Song *et al.*，2016；Jia *et al.*，2022)，表明夏日哈木岩体虽然经历了晚期熔离，但其原生岩浆具有高氧逸度和富硫的特征(Song *et al.*，2016；Chen *et al.*，2021；陈文等，2025)，且在岩浆演化过程中经历地壳物质的混染，富硫成分的加入降低了硫的溶解度，造成了大量硫酸盐被还原为硫化物，最终熔离成矿。

在岩浆演化早期，不相容元素 Cu 与 Zr 在残余熔体中共同富集，维持其比值相对稳定。然而，一旦岩浆达到硫饱和并发生硫化物熔离，强亲硫元素 Cu 将被大量分配至硫化物

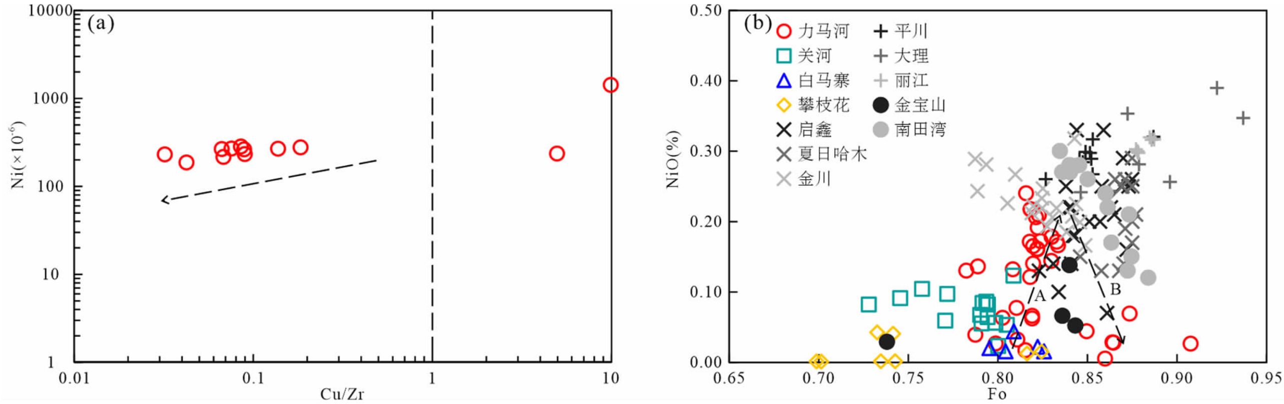

图 14 橄榄石 Cu/Zr-Ni(a)相关图和 Fo-NiO(b)相关图

Fig. 14 Correlation plots of olivine Cu/Zr vs. Ni (a) and Fo vs. NiO (b)

相,而亲石元素 Zr 则继续在硅酸盐熔体中富集,造成残余熔体及其中结晶橄榄石的 Cu/Zr 比值急剧下降。橄榄石的 Cu/Zr 比值与 Ni 含量之间的关系为揭示硫化物熔离提供了关键地球化学依据(Barnes *et al.*, 1988; Li and Naldrett, 1999)。力马河岩体橄榄石所表现出的低 Cu/Zr 值(尤其 <1)与 Ni 含量的负相关性,清晰地记录了其硫化物熔离事件:力马河岩体可能经历了两阶段熔离过程。第一次深部通道熔离,岩浆在深部上升通道中经历地壳混染导致发生早期硫化物熔离,岩浆强烈亏损 Ni,这是橄榄石低 Ni 的原因(图 14b 曲线 B);而其 Ni 含量随着结晶作用的进行而呈现升高趋势(图 14b 曲线 A),可以用第二次熔离来解释:亏损 Ni 的岩浆侵位后,在结晶分异过程中再次达到硫饱和,发生原地熔离,橄榄石与硫化物熔体发生再平衡,造成 Ni 含量升高。这次熔离主要影响残余熔体的 Cu/Zr 比值,形成了 Fo-NiO 图解上的特定趋势(图 14b 曲线 AB)以及 Cu/Zr 与 Ni 的负相关关系(图 14a)。

力马河岩体中的硫化物主要赋存于橄榄岩相内,以填隙形式分布于橄榄石颗粒之间或呈包裹体形式被橄榄石包裹(图 3g, h)。值得注意的是,包裹硫化物珠滴的橄榄石通常具有较高的 Fo 牌号,这一结构特征表明,硫化物熔离事件发生于母岩浆演化的早期阶段,即镁橄榄石结晶的同时或稍早。从整体矿石结构来看,硫化物多呈浸染状和团块状产出,这进一步证实了硫化物熔离作用先于橄榄石主体分离结晶发生。这种早期的通道熔离机制有效地富集了金属元素,预示着力马河岩体深部依然具备形成高品位岩浆硫化物矿床的良好潜力。

6 结论

(1)地球化学参数指示:橄榄石 Fo 值、Mn/Zn 比值、V/Sc 比值、10000×Zn/Fe 值与 Mn 含量可有效约束镍矿岩浆源区性质;橄榄石 Li 含量示踪地壳混染作用;橄榄石 Ni 含量与 Cu/Zr 比值限定硫化物熔离发生时期。单斜辉石 Al_2O_3、SiO_2 含量判别母岩浆碱性系列;SiO_2、Na_2O、TiO_2 含量揭示其分异环境。

(2)力马河岩体岩浆源区为深部还原性石榴子石橄榄岩地幔。力马河超镁铁质母岩浆为高镁玄武质岩浆,镁铁质母岩浆为拉斑玄武质岩浆,同属低 Ti 玄武质岩浆系列。单斜辉石具亚碱性系列特征,指示岩浆形成于拉斑环境,具 OIB 属性但相容元素更富集,反映地幔柱垂向非均质性。

(3)力马河岩体经历二阶段硫化物熔离:早期深部熔离致橄榄石 Ni 严重亏损(NiO<0.25%);侵位过程地壳混染触发原地熔离,Cu/Zr 比值骤降,硫化物熔离后与橄榄石再平衡导致 Ni 含量升高。硫化物包裹体见于高 Fo 橄榄石中,证实熔离始于早期。成矿受地幔柱源区、地壳混染与熔离时序耦合控制。

致谢 本文野外工作得到了四川省第五地质大队和中国地质调查局四川军民融合地质调查中心的无私支持和帮助;实验工作得到了中国地质科学院矿产资源研究所的陈振宇、刘春花等多位老师的指导;匿名审稿专家给予了宝贵的指导和修改建议,在此一并致以最诚挚的谢意。

References

Ai Y, Zhang ZC, Wang FS, Hao YL, Zhao L and Yang TZ. 2006. Trace element and Sr-Nd-Pb-O isotopic systems of the Panzhihua layered gabbro intrusion: Constraints on the mantle source regions and origin of V-Ti-Fe oxide deposit. Acta Geologica Sinica, 80(7): 995-1004 (in Chinese with English abstract)

Arndt NT, Czamanske GK, Walker RJ, Chauvel C and Fedorenko V. 2003. Geochemistry and origin of the intrusive hosts of the Noril'sk-Talnakh Cu-Ni-PGE sulfide deposits. Economic Geology, 98(3): 495-515

Bai ZJ, Zhong H and Zhu WG. 2019. Redox state of mantle-derived magma and constraints on the genesis of magmatic deposits. Acta Petrologica Sinica, 35(1): 204-214 (in Chinese with English abstract)

Baker J, Matthews A, Mattey D, Rowley D and Xue F. 1997. Fluid-rock interactions during ultra-high pressure metamorphism, Dabie Shan, China. Geochimica et Cosmochimica Acta, 61(8): 1685-1696

Bao J. 2024. Genesis of the Xiarihamu super-large magmatic Ni-Co sulfide deposit in the East Kunlun orogenic belt. Ph. D. Dissertation. Lanzhou: Lanzhou University (in Chinese with English abstract)

Barnes SJ, Boyd R, Korneliussen A, Nilsson LP, Often M, Pedersen RB and Robins B. 1988. The use of mantle normalization and metal ratios in discriminating between the effects of partial melting, crystal fractionation and sulphide segregation on platinum-group elements, gold, nickel and copper: Examples from Norway. In: Prichard HM, Potts PJ, Bowles JFW and Cribb SJ (eds.). Geo-Platinum 87. Dordrecht: Springer, 113-143

Barnes SJ and Lightfoot PC. 2005. Formation of magmatic nickel sulfide deposits and processes affecting their copper and platinum group element contents. In: Hedenquist JW, Thompson JFH, Goldfarb RJ and Richards JP (eds.). One Hundredth Anniversary Volume. Society of Economic Geologists, 178-213

Barnes SJ, Godel B, Gürer D, Brenan JM, Robertson J and Paterson D. 2013. Sulfide-olivine Fe-Ni exchange and the origin of anomalously Ni rich magmatic sulfides. Economic Geology, 108(8): 1971-1982

Brenan JM, Ryerson FJ and Shaw HF 1998. The role of aqueous fluids in the slab-to-mantle transfer of boron, beryllium, and lithium during subduction: Experiments and models. Geochimica et Cosmochimica Acta, 62: 3337-3347

Brenan JM and Caciagli NC. 2000. Fe-Ni exchange between olivine and sulphide liquid: Implications for oxygen barometry in sulphide-saturated magmas. Geochimica et Cosmochimica Acta, 64(2): 307-320

Cai WC. 2021. Characteristics of olivine phenocrysts of the picritics in the Emeishan large igneous province and its implications for mantle source. Ph. D. Dissertation. Beijing: China University of Geosciences (in Chinese with English abstract)

Chai G and Naldrett AJ. 1992. Characteristics of Ni-Cu-PGE mineralization and genesis of the Jinchuan deposit, Northwest China. Economic Geology, 87(6): 1475-1495

Chen LM, Song XY, Hu RZ, Yu SY, Yi JN, Kang J and Huang KJ. 2021. Mg-Sr-Nd isotopic insights into petrogenesis of the Xiarihamu mafic-ultramafic intrusion, northern Tibetan Plateau, China. Journal of Petrology, 62(2): egaa113

Chen W, Chen LM, Yu SY, Li DP, Wu SK and Wang ZA. 2025. The formation of magmatic Ni-Co sulfide deposits in the East Kunlun Orogen: Constraints from geochemical compositions of olivine and whole-rock S isotopic data. Acta Petrologica Sinica, 41(2): 453-475 (in Chinese with English abstract)

Chin EJ, Lee CTA and Barnes JD. 2014. Thickening, refertilization, and the deep lithosphere filter in continental arcs: Constraints from major and trace elements and oxygen isotopes. Earth and Planetary Science Letters, 397: 184-200

Chung SL and Jahn B. 1995. Plume-lithosphere interaction in generation of the Emeishan flood basalts at the Permian-Triassic boundary. Geology, 23(10): 889-892

Dang YX. 2018. Study on the metallogenesis of the Baima ultra-large V-Ti-magnetite deposit in the Emeishan large igneous province, SW China. Master Degree Thesis. Lanzhou: Lanzhou University (in Chinese with English abstract)

DePaolo DJ. 1981. Trace element and isotopic effects of combined wallrock assimilation and fractional crystallization. Earth and Planetary Science Letters, 53(2): 189-202

Evans-Lamswood DM, Butt DP, Jackson RS, Lee DV, Muggridge MG and Wheeler DHC. 2000. Physical controls associated with the distribution of sulfides in the Voisey's Bay Ni-Cu-Co deposit, Labrador. Economic Geology, 95(4): 749-769

Faggart Jr BE, Basu AB and Tatsumoto M. 1985. Origin of the Sudbury Complex by meteoritic impact: Neodymium isotopic evidence. Science, 230(4724): 436-439

Foley SF, Prelevic D, Rehfeldt T and Jacob DE. 2013. Minor and trace elements in olivines as probes into early igneous and mantle melting processes. Earth and Planetary Science Letters, 363: 181-191

Gao WY. 2018. Microstructure and trace element composition of minerals and their indication for ore-forming process in the Panzhihua layered intrusion, SW China. Ph. D. Dissertation. Shenyang: Northeastern University (in Chinese with English abstract)

Guan T, Huang ZL, Xu DR, Zhang ZL, Yan ZF and Xu C. 2006. Lithogeochemistry of the sulfide-bearing mafic-ultramafic rock at Baimazhai, Jinping, Southern Yunnan. Chinese Journal of Geology, 41(3): 441-454 (in Chinese with English abstract)

Guilin Institute of Metallurgical Geology, No. 601 Geological Brigade, Sichuan Metallurgical Geological Exploration Bureau and No. 901 Mine of Sichuan Metallurgical Bureau. 1974. Study on the Limahe sulfide copper-nickel Deposit. In: Division of Geology and Mineral Resources, Institute of Geological Sciences (ed.). Special Volume on the Geology and Mineral Resources of Copper, Nickel, Cobalt, and Platinum (Volume 2). Beijing: Geological Publishing House, 51-95 (in Chinese)

Guo YF, She YW, Li SS, Zhu ZY, Xie QH and He HL. 2025. In-situ Sr isotope and trace element of clinopyroxene from the Hongge intrusion in the Pan-Xi region: Constraints on the formation of the giant Fe-Ti oxide ores. Earth Science Frontiers, 1-24. https://doi.org/10.13745/j.esf.yx.2025.1.25 (in Chinese with English abstract)

Haggerty SE. 1991. Oxide textures-a mini-atlas. In: Lindsley DH (ed.). Oxide Minerals. Washington: Mineralogical Society of America, 129-220

He B, Xu YG, Xiao L, Wang KM and Sha SL. 2003. Generation and spatial distribution of the Emeishan large igneous province: New evidence from stratigraphic records. Acta Geologica Sinica, 77(2): 194-202 (in Chinese with English abstract)

Howarth GH and Harris C. 2017. Discriminating between pyroxenite and peridotite sources for continental flood basalts (CFB) in southern Africa using olivine chemistry. Earth and Planetary Science Letters, 475: 143-151

Jeffcoate AB, Elliott T, Kasemann SA, Ionov D, Cooper K and Brooker R. 2007. Li isotope fractionation in peridotites and mafic melts. Geochimica et Cosmochimica Acta, 71(1): 202-218

Jia LH, Chen Y, Su B, Mao Q and Zhang D. 2022. Oxygen-fugacity evolution of magmatic Ni-Cu sulfide deposits in East Kunlun: Insights from Cr-spinel composition. American Mineralogist, 107(10): 1968-1981

Jiang CY, Ling JL, Zhou W, Du W, Wang ZX, Fan YZ, Song YF and Song ZB. 2015. Petrogenesis of the Xiarihamu Ni-bearing layered mafic-ultramafic intrusion, East Kunlun: Implications for its extensional island arc environment. Acta Petrologica Sinica, 31(4): 1117-1136 (in Chinese with English abstract)

Lee CTA, Luffi P, Le Roux V, Dasgupta R, Albaréde F and Leeman WP. 2010. The redox state of arc mantle using Zn/Fe systematics. Nature, 468(7324): 681-685

Li C and Naldrett AJ. 1999. The geology and petrology of the Voisey's Bay intrusion: reaction of olivine with trapped sulfide and silicate liquids. Lithos, 47: 1-31

Li CS and Ripley EM. 2011. The giant Jinchuan Ni-Cu-(PGE) deposit: Tectonic setting, magma evolution, ore genesis, and exploration implications. In: Li CS and Ripley EM (eds.). Magmatic Ni-Cu and PGE Deposits: Geology, Geochemistry, and Genesis. Society of Economic Geologists, 163-180

Li CS, Ripley EM, Thakurta J, Stifter EC and Qi L. 2013. Variations of olivine Fo-Ni contents and highly chalcophile element abundances in arc ultramafic cumulates, southern Alaska. Chemical Geology, 351: 15-28

Li HB. 2012. Mantle plume geodynamic significances of the Emeishan large igneous province: Evidence from mafic dykes, geochemistry and stratigraphic records. Ph. D. Dissertation. Beijing: China University of Geosciences (in Chinese with English abstract)

Li WY. 2015. Metallogenic geological characteristics and newly discovered orebodies in Northwest China. Geology in China, 42(3): 365-380 (in Chinese with English abstract)

Li WY. 2022. Study of ore-forming theoretical innovation and prospecting breakthrough of magmatic copper-nickel-cobalt sulfide deposits in China. Journal of Geomechanics, 28(5): 793-820 (in Chinese with English abstract)

Li Y. 2010. Studies of petrology and geochemistry on the Limahe mafic-ultramafic intrusion in Panxi district, SW China. Master Degree Thesis. Beijing: China University of Geosciences (in Chinese with English abstract)

Li YG. 2007. The screening of Ni-Cu-PGE sulfide ores prospecting target area in Pan-xi area in Sichuan Province based on "3S" technology. Ph. D. Dissertation. Chengdu: Chengdu University of Technology (in Chinese with English abstract)

Li ZZ, Wang YL, Wang MX, Jiao JG and Xia MZ. 2023. The nature of mantle source and the process of sulfide segregation of the Xiarihamu No. Ⅰ intrusion: Insights from olivine, chalcophile elemental and sulfur isotopic compositions. Acta Geologica Sinica, 97(10): 3326-3346 (in Chinese with English abstract)

Liu YG, Li WY, Lü XB, Huo YH and Zhang B. 2017. The Pobei Cu-Ni and Fe ore deposits in NW China are comagmatic evolution products: Evidence from ore microscopy, zircon U-Pb chronology and geochemistry. Geologica Acta, 15(1): 37-50

Lo CH, Chung SL, Lee TY and Wu GY. 2002. Age of the Emeishan flood magmatism and relations to Permian-Triassic boundary events. Earth and Planetary Science Letters, 198(3-4): 449-458

Lu YG, Michael Lesher C and Deng J. 2019. Geochemistry and genesis of magmatic Ni-Cu-(PGE) and PGE-(Cu)-(Ni) deposits in China. Ore Geology Reviews, 107: 863-887

Luan Y, Song XY, Chen LM, Zheng WQ, Zhang XQ, Yu SY, She YW, Tian XL and Ran QY. 2014. Key factors controlling the accumulation of the Fe-Ti oxides in the Hongge layered intrusion in the Emeishan Large Igneous Province, SW China. Ore Geology Reviews, 57: 518-538

Luo WJ. 2013. Comparisons between ore-bearing and barren mafic-ultramafic intrusions in the Emeishan large igneous province, southwest China. Ph. D. Dissertation. Beijing: China University of Geosciences (in Chinese with English abstract)

Luo YN. 1985. Advances in the understanding of the Panxi Paleorift. Geology in China, 1(1): 27-31 (in Chinese)

Luo YY. 2025. Petrogenesis of basalts and picrites in the Lijiang area of the ELIP inner zone. Master Degree Thesis. Guilin: Guilin University of Technology (in Chinese with English abstract)

Macdonald R, Rogers NW, Fitton JG, Black S and Smith M. 2001. Plume-lithosphere interactions in the generation of the basalts of the Kenya Rift, East Africa. Journal of Petrology, 42(5): 877-900

Maier WD, Li CS and De Waal SA. 2001. Why are there no major Ni-Cu sulfide deposits in large layered mafic-ultramafic intrusions? The Canadian Mineralogist, 39(2): 547-556

Mao YJ, Schoneveld L, Barnes SJ, Williams MJ, Su BX, Ruprecht P, Evans NJ and Qin KZ. 2022. Coupled Li-P zoning and trace elements of olivine from magmatic Ni-Cu Deposits: Implications for postcumulus re-equilibration in olivine. Journal of Petrology, 63(3): egac018

Mao YJ, Wu ST, Jia LH, Qin KZ and Zhai MG. 2024. Trace elements in olivine: Analysis, geochemical behavior, and case studies. Acta Petrologica Sinica, 40(10): 3160-3190 (in Chinese with English abstract)

Marschall HR, Wanless VD, Shimizu N, von Strandmann PAEP, Elliott T and Monteleone BD. 2017. The boron and lithium isotopic composition of mid-ocean ridge basalts and the mantle. Geochimica et Cosmochimica Acta, 207: 102-138

Mavrogenes JA and O'Neill HSC. 1999. The relative effects of pressure, temperature and oxygen fugacity on the solubility of sulfide in mafic magmas. Geochimica et Cosmochimica Acta, 63(7-8): 1173-1180

Mo XX. 2019. Magmatism and deep geological process. Earth Science, 44(5): 1487-1493 (in Chinese with English abstract)

Morimoto N, Fabries J, Ferguson AK, Ginzburg IV, Ross M, Seifert FA, Zussman J, Aoki K and Gottardi G. 1988. Nomenclature of pyroxenes. American Mineralogist, 73: 1123-1133

Naldrett AJ, Lightfoot PC, Fedorenko V, Doherty W and Gorbachev NS. 1992. Geology and geochemistry of intrusions and flood basalts of the Noril'sk region, USSR, with implications for the origin of the Ni-Cu ores. Economic Geology, 87(4): 975-1004

Naldrett AJ. 1989. Magmatic Sulfide Deposits. New York: Oxford University Press

Naldrett AJ. 1999. World-class Ni-Cu-PGE deposits: Key factors in their genesis. Mineralium Deposita, 34(3): 227-240

Naldrett AJ. 2004. Magmatic Sulfide Deposits: Geology, Geochemistry and Exploration. Berlin: Springer, 1-727

Naldrett AJ. 2010. Secular variation of magmatic sulfide deposits and their source magmas. Economic Geology, 105(3): 669-688

Naldrett AJ. 2011. Fundamentals of magmatic sulfide deposits. In: Li CS and Ripley EM (eds.). Reviews in Economic Geology: Magmatic Ni-Cu and PGE Deposits: Geology, Geochemistry, and Genesis. Society of Economic Geologists, 1-50

Neal CR, Mahoney JJ and Chazey Ⅲ WJ. 2002. Mantle sources and the highly variable role of continental lithosphere in basalt petrogenesis of the Kerguelen Plateau and Broken Ridge LIP: Results from ODP Leg 183. Journal of Petrology, 43(7): 1177-1205

Pang KN, Zhou MF, Qi L, Shellnutt G, Wang CY and Zhao DG. 2010. Flood basalt-related Fe-Ti oxide deposits in the Emeishan large igneous province, SW China. Lithos, 119(1-2): 123-136

Pang ZZ, Xia MZ, Wang YQ, Man Y, Xia ZD and Zhang HD. 2025. The nature of the mantle source and exploration implications of the Qixin intrusion, Beishan, Xinjiang: Insights from olivine composition. Geological Bulletin of China, 44(10): 2003-2018 (in Chinese with English abstract)

Peng L. 2023. Geochemistry and magmatic evolution of the western intrusion in the Jinchuan Cu-Ni sulfide deposit. Master Degree Thesis. Changsha: Central South University (in Chinese with English abstract)

Pirajno F, Hocking RM, Reddy SM and Jones AJ. 2009. A review of the geology and geodynamic evolution of the Palaeoproterozoic Earaheedy Basin, Western Australia. Earth-Science Reviews, 94(1-4): 39-77

Prelević D, Jacob DE and Foley SF. 2013. Recycling plus: A new recipe for the formation of Alpine-Himalayan orogenic mantle lithosphere. Earth and Planetary Science Letters, 362: 187-197

Qiu JX and Liao QA. 1996. Petrogenesis and Cpx mineralchemistry of Cenozoic basalts from Zhejiang and Fujian of Eastern China. Volcanology & Mineral Resources, 17(1-2): 16-25 (in Chinese with English abstract)

Ran FQ, Zhong KH and Lu MX. 2015. Research of Huili County Limahe copper nickel mineralization and metallogenic model of elements. Sichuan Nonferrous Metals, (4): 43-46 (in Chinese with English abstract)

Ren ZY, Wu YD, Zhang L, Nichols ARL, Hong LB, Zhang YH, Zhang Y, Liu JQ and Xu YG. 2017. Primary magmas and mantle sources of Emeishan basalts constrained from major element, trace element and Pb isotope compositions of olivine-hosted melt inclusions. Geochimica et Cosmochimica Acta, 208: 63-85

Roeder PL and Emslie RF. 1970. Olivine-liquid equilibrium. Contributions to Mineralogy and Petrology, 29(4): 275-289

Rollinson HR. 1993. Using Geochemical Data: Evaluation, Presentation, Interpretation. London: Routledge, 1-352

Ross JR and Travis GA. 1981. The nickel sulfide deposits of Western Australia in global perspective. Economic Geology, 76(6): 1291-1329

Rudnick RL and Gao S. 2003. Composition of the continental crust. In: Rudnick RL (ed.). Treatise on Geochemistry. Amsterdam: Elsevier, 659

Shellnutt JG and Zhou MF. 2007. Permian peralkaline, peraluminous and metaluminous A-type granites in the Panxi district, SW China: Their relationship to the Emeishan mantle plume. Chemical Geology, 243(3-4): 286-316

Shellnutt JG, Zhou MF and Zellmer GF. 2009. The role of Fe-Ti oxide crystallization in the formation of A-type granitoids with implications for the Daly gap: An example from the Permian Baima igneous complex, SW China. Chemical Geology, 259(3-4): 204-217

Shellnutt JG, Pham TT, Denyszyn SW, Yeh MW and Tran TA. 2020. Magmatic duration of the Emeishan large igneous province: Insight from northern Vietnam. Geology, 48(5): 457-461

Søager N, Portnyagin M, Hoernle K, Holm PM, Hauff F and Garbe-Schönberg D. 2015. Olivine major and trace element compositions in southern Payenia basalts, Argentina: Evidence for pyroxenite-peridotite melt mixing in a back-arc setting. Journal of Petrology, 56(8): 1495-1518

Sobolev AV, Hofmann AW, Sobolev SV and Nikogosian IK. 2005. An olivine-free mantle source of Hawaiian shield basalts. Nature, 434(7033): 590-597

Sobolev AV, Hofmann AW, Kuzmin DV, Yaxley GM, Arndt NT, Chung SL, Danyushevsky LV, Elliott T, Frey FA, Garcia MO, Gurenko AA, Kamenetsky VS, Kerr AC, Krivolutskaya NA, Matvienkov VV, Nikogosian IK, Rocholl A, Sigurdsson IA, Sushchevskaya NM and Teklay M. 2007. The amount of recycled crust in sources of mantle-derived melts. Science, 316(5823): 412-417

Song XY, Hou ZQ, Cao ZM, Lu JR, Wang YL, Zhang CJ and Li YG. 2001. Geochemical characteristics and period of the Emei igneous province. Acta Geologica Sinica, 75(4): 498-506 (in Chinese with English abstract)

Song XY, Zhou MF, Tao Y and Xiao JF. 2008. Controls on the metal compositions of magmatic sulfide deposits in the Emeishan large igneous province, SW China. Chemical Geology, 253(1-2): 38-49

Song XY, Yi JN, Chen LM, She YW, Liu CZ, Dang XY, Yang QA and Wu SK. 2016. The giant Xiarihamu Ni-Co sulfide deposit in the East Kunlun orogenic belt, northern Tibet Plateau, China. Economic Geology, 111(1): 29-55

Spera FJ and Bohrson WA. 2001. Energy-constrained open-system magmatic processes I: General model and energy-constrained assimilation and fractional crystallization (EC-AFC) formulation. Journal of Petrology, 42(5): 999-1018

Sun SS and McDonough WF. 1989. Chemical and isotopic systematics of oceanic Basalts: Implications for mantle composition and processes. In: Saunder AD and Norry MJ (eds.). Magmatism in the Ocean Basins. Geological Society, London, Special Publications, 42: 313-345

Sun SS, Wallace DA, Hoatson DM, Glikson AY and Keays RR. 1991. Use of geochemistry as a guide to platinum group element potential of mafic-ultramafic rocks: Examples from the west Pilbara Block and Halls Creek Mobile Zone, Western Australia. Precambrian Research, 50(1-2): 1-35

Tang ZL, Yan HQ, Jiao JG and Li XH. 2006. New classification of magmatic sulfide deposits in China and ore-forming processes of small intrusive bodies. Mineral Deposits, 25(1): 1-9 (in Chinese with English abstract)

Tang ZL, Qian ZZ, Jiang CY, Yan HQ, Jiao JG, Liu MW, Xu ZH, Xu G and Wang YL. 2011. Trends of research in exploration of magmatic sulfide deposits and small intrusions metallogenic system. Journal of Earth Sciences and Environment, 33(1): 1-9 (in Chinese with English abstract)

Tao Y, Hu RZ, Qi L and Luo TY. 2007. Geochemical characteristics and metallogenesis of the Limahe mafic-ultramafic intrusion, Sichuan. Acta Petrologica Sinica, 23(11): 2785-2800 (in Chinese with English abstract)

Tao Y, Hu RZ, Qu WJ and Du AD. 2008. Re-Os isotope study of sulfide and olivine pyroxenite in the Limahe nickle deposit, Sichuan Province. Acta Geologica Sinica, 82(9): 1292-1304 (in Chinese with English abstract)

Wang LG. 2015. Characteristics and metallogenic prospect of the Jinbaoshan mafic-ultramafic complex, Yunnan Province. Master Degree Thesis. Chengdu: Chengdu University of Technology (in Chinese with English abstract)

Wang M, Zhang ZC, Hou T and Luo WJ. 2011. Geochronology and geochemistry of the Dabanshan intrusion in Panxi district and its constraints on the metallogenesis of Cu-Ni sulfide deposits. Acta Petrologica Sinica, 27(9): 2665-2678 (in Chinese with English abstract)

Wang Y. 2008. Origin of the Permian Baimazhai magmatic Ni-Cu-(PGE) sulfide deposits, Yunnan: Implications for the relationship of crustal contamination and mineralization. Bulletin of Mineralogy, Petrology and Geochemistry, 27(4): 332-343 (in Chinese with English abstract)

Xiao L, Xu YG, Mei HJ, Zheng YF, He B and Pirajno F. 2004. Distinct mantle sources of low-Ti and high-Ti basalts from the western Emeishan large igneous province, SW China: Implications for plume-lithosphere interaction. Earth and Planetary Science Letters, 228(3-4): 525-546

Xu R, Liu YS and Lambart S. 2020. Melting of a hydrous peridotite mantle source under the Emeishan large igneous province. Earth-Science Reviews, 207: 103253

Xu WB. 2023. The Ni-Co metallogenic magmatism of Qixin mafic-ultramafic complex in Beishan, China: Constraints from C-He-Ne-Ar isotopes. Master Degree Thesis. Lanzhou: Lanzhou University (in Chinese with English abstract)

Xu YG, Chung SL, Jahn BM and Wu GY. 2001. Petrologic and geochemical constraints on the petrogenesis of Permian-Triassic Emeishan flood basalts in southwestern China. Lithos, 58(3-4): 145-168

Xu YG, He B, Chung SL, Menzies MA and Frey FA. 2004. Geologic, geochemical, and geophysical consequences of plume involvement in the Emeishan flood-basalt province. Geology, 32(10): 917-920

Xu YG and He B. 2007. Thick, high-velocity crust in the Emeishan large igneous province, southwestern China: Evidence for crustal groh by magmatic underplating or intraplating. In: Foulger GR and Jurdy DM (eds.). Plates, Plumes and Planetary Processes. Geological Society of America, 841-858

Xu ZH, Tang ZL and Cai KQ. 1998. Estimation for chemical composition of parent magma of Jinchuan Cu-Ni (PGE) magmatic sulfide deposit. Geoscience, 12(4): 506-514

Xue SC, Li CS, Wang QF, Ripley EM and Yao ZS. 2019. Geochronology, petrology and Sr-Nd-Hf-S isotope geochemistry of the newly-discovered Qixin magmatic Ni-Cu sulfide prospect, southern Central Asian Orogenic Belt, NW China. Ore Geology Reviews, 111: 103002

Yao JD. 1988. On the Genesis of Cu-(Pt)-Ni Sulfide Deposits in Xichang Region. Chongqing: Chongqing Publishing House (in Chinese)

Yao JH, Zhu WG, Li CS, Zhong H, Yu SY, Ripley EM and Bai ZJ. 2019. Olivine O isotope and trace element constraints on source variation of picrites in the Emeishan flood basalt province, SW China. Lithos, 338-339: 87-98

You MX, Zhang ZW, Liu JM, Zhang JW, Wang YL and Qian B. 2017. Geochemistry of mafic-ultramafic intrusions and Cu-Ni-(PGE) sulfide deposits in Panxi Region, China. Northwestern Geology, 50(3): 146-161 (in Chinese with English abstract)

Zhang FF. 2023. Study on the multi-phase diagenetic mineralization of Xiarihamu Ni-Co sulfide deposit. Master Degree Thesis. Hefei: Hefei University of Technology (in Chinese with English abstract)

Zhang L, Ren ZY and Wang Y. 2017. Melt inclusions in the olivine from the Nantianwan intrusion: Implications for the parental magma of Ni-Cu-(PGE) sulfide-bearing mafic-ultramafic intrusions of the ~260Ma Emeishan large igneous province (SW China). Journal of Asian Earth Sciences, 134(72-85): 1367-9120

Zhang L, Ren ZY and Zhang L. 2022. The nature of mantle source of the Pingchuan picrites in the Emeishan Large Igneous Province: Constrains from the trace element composition of olivines. Geotectonica et Metallogenia, 46(1): 112-131 (in Chinese with English abstract)

Zhang YX. 1982. A major N-S trending tectonic unit in southwestern China: The Panzhihua-Xichang Rift Zone. Acta Geologica Sichuan, 3(Suppl. 1): 11-24, 58 (in Chinese)

Zhang ZB, Li WY, Zhang ZW, Liu YG, Qian B, Wang YL, Zhang JW, Wang BL and Zhang HC. 2016. Characteristics of chromian spinels from the Xiarihamu magmatic Ni-Cu sulfide ore deposit in the Eastern

Kunlun Orogenic Belt, Northwest China and their implication. Bulletin of Mineralogy, Petrology and Geochemistry, 35(5): 966-975 (in Chinese with English abstract)
Zhang ZC, Mahoney JJ, Mao JW and Wang FS. 2006. Geochemistry of picritic and associated basalt flows of the western Emeishan flood basalt province, China. Journal of Petrology, 47(10): 1997-2019
Zhang ZC, Mao JW, Saunders AD, Ai Y, Li Y and Zhao L. 2009. Petrogenetic modeling of three mafic-ultramafic layered intrusions in the Emeishan large igneous province, SW China, based on isotopic and bulk chemical constraints. Lithos, 113(3-4): 369-392
Zhang ZW, Wang YL, Shao J and Li WY. 2021. Metallogenic characteristics of Xiarihamu super-large magmatic nickel-cobalt sulfide deposit in eastern Kunlun Orogenic Belt. Mineral Deposits, 40(6): 1230-1247 (in Chinese with English abstract)
Zhao BB, Deng YF, Zhou TF, Yuan F, Zhang DY, Deng G, Li WD and Li Y. 2018. Petrogenesis of the Baixintan Ni-Cu sulfide-bearing mafic-ultramafic intrusion, East Tianshan: Evidence from geochronology, petrogeochemistry and Sr-Nd isotope. Acta Petrologica Sinica, 34(9): 2733-2753 (in Chinese with English abstract)
Zhao Y, Xue CJ, Zhao XB, Yang YQ and Ke JJ. 2015. Magmatic Cu-Ni sulfide mineralization of the Huangshannan mafic-untramafic intrusion, Eastern Tianshan, China. Journal of Asian Earth Sciences, 105: 155-172
Zhao Y. 2020. Study on the formation mechanism of the Panzhihua basic-ultrabasic dyke in the Emeishan large igneous province, SW China. Master Degree Thesis. Lanzhou: Lanzhou University (in Chinese with English abstract)
Zhong H, Hu RZ, Wilson AH and Zhu WG. 2005. Review of the link between the Hongge layered intrusion and Emeishan flood basalts, Southwest China. International Geology Review, 47(9): 971-985
Zhong X. 2019. Research on the metallogenic mechanism of the "Panzhihua-type" vanadium-titanium magnetite deposit. Master Degree Thesis. Chengdu: Southwest Petroleum University (in Chinese with English abstract)
Zhou MF, Robinson PT, Lesher CM, Keays RR, Zhang CJ and Malpas J. 2005. Geochemistry, petrogenesis and metallogenesis of the Panzhihua gabbroic layered intrusion and associated Fe-Ti-V-oxide deposits, Sichuan Province, SW China. Journal of Petrology, 46(11): 2253-2280
Zhou MF, Arndt NT, Malpas J, Wang CY and Kennedy AK. 2008. Two magma series and associated ore deposit types in the Permian Emeishan large igneous province, SW China. Lithos, 103(3-4): 352-368
Zhu D, Luo TY, Gao ZM and Zhu CM. 2003. Differentiation of the Emeishan flood basalts at the base and throughout the crust of Southwest China. International Geology Review, 45(5): 471-477
Zhu FL, Bai M and Tao Y. 2017. Lithogeochemical characteristics and metallogenic mechanism of the Hetaoshu rich-PGE magmatic sulfide deposit in the Xiaoguanhe region, Panxi. Acta Petrologica Sinica, 33(7): 2225-2240 (in Chinese with English abstract)

附中文参考文献

艾羽，张招崇，王福生，郝艳丽，赵莉，杨铁铮. 2006. 攀枝花层状辉长质岩体的微量元素和锶钕铅氧同位素系统：地幔源区和矿床成因的证据. 地质学报，80(7)：995-1004
柏中杰，钟宏，朱维光. 2019. 幔源岩浆氧化还原状态及对岩浆矿床成矿的制约. 岩石学报，35(1)：204-214
鲍坚. 2024. 东昆仑造山带夏日哈木超大型岩浆镍钴硫化物矿床成因. 博士学位论文. 兰州：兰州大学
蔡文昌. 2021. 峨眉山大火成岩省苦橄岩橄榄石特征及对地幔源区的指示. 博士学位论文. 北京：中国地质大学(北京)
陈文，陈列锰，于宋月，李大鹏，吴树宽，王治安. 2025. 东昆仑造山带岩浆 Ni-Co 硫化物矿床成矿作用：橄榄石成分和全岩 S 同位素制约. 岩石学报，41(2)：453-475
党永西. 2018. 峨眉山大火成岩省白马超大型钒钛磁铁矿矿床成矿作用研究. 硕士学位论文. 兰州：兰州大学
高文元. 2018. 攀枝花层状侵入体中矿物微观结构和微量元素对成矿过程的指示. 博士学位论文. 沈阳：东北大学
管涛，黄智龙，许德如，张振亮，严再飞，许成. 2006. 云南金平白马寨含矿镁铁-超镁铁岩体岩石地球化学. 地质科学，41(3)：441-454
桂林冶金地质研究所，四川冶金地质勘探公司 601 队，四川冶金局 901 矿. 1974. 力马河硫化物铜镍矿床研究. 地质科学研究院地质矿产所编：铜镍钴铂地质矿产专集(第二集). 北京：地质出版社，51-95
郭艳峰，佘宇伟，李珊珊，朱志勇，谢秋红，何海龙. 2025. 攀西红格岩体单斜辉石 Sr 同位素和微量元素组成制约钒钛磁铁矿床成因. 地学前缘，1-24. https://doi.org/10.13745/j.esf.yx.2025.1.25
何斌，徐义刚，肖龙，王康明，沙绍礼. 2003. 峨眉山大火成岩省的形成机制及空间展布：来自沉积地层学的新证据. 地质学报，77(2)：194-202
姜常义，凌锦兰，周伟，杜玮，王子玺，范亚洲，宋艳芳，宋忠宝. 2015. 东昆仑夏日哈木镁铁质-超镁铁质岩体岩石成因与拉张型岛弧背景. 岩石学报，31(4)：1117-1136
李宏博. 2012. 峨眉山大火成岩省地幔柱动力学：基性岩墙群、地球化学及沉积地层学证据. 博士学位论文. 北京：中国地质大学(北京)
李文渊. 2015. 中国西北部成矿地质特征及找矿新发现. 中国地质，42(3)：365-380
李文渊. 2022. 中国岩浆铜镍钴硫化物矿床成矿理论创新和找矿突破. 地质力学学报，28(5)：793-820
李莹. 2010. 攀西地区力马河镁铁-超镁铁质岩体的岩石学和地球化学研究. 硕士学位论文. 北京：中国地质大学(北京)
李佑国. 2007. 基于"3S"技术的攀西地区铜镍铂族元素矿床找矿靶区筛选. 博士学位论文. 成都：成都理工大学
李中州，王亚磊，王梦玺，焦建刚，夏明哲. 2023. 夏日哈木超大型镍矿Ⅰ号岩体地幔源区性质和硫化物熔离过程：来自橄榄石成分、亲铜元素和硫同位素的约束. 地质学报，97(10)：3326-3346
罗阳阳. 2025. 峨眉山大火成岩省内带丽江玄武岩-苦橄岩岩石成因探究. 硕士学位论文. 桂林：桂林理工大学
骆文娟. 2013. 峨眉山大火成岩省无矿基性超基性岩体与含矿岩体对比研究. 博士学位论文. 北京：中国地质大学(北京)
骆耀南. 1985. 攀西古裂谷研究中的认识和进展. 中国地质，1(1)：27-31
毛亚晶，吴石头，贾丽辉，秦克章，翟明国. 2024. 橄榄石微量元素：分析、地球化学行为与地球科学应用. 岩石学报，40(10)：3160-3190
莫宣学. 2019. 岩浆作用与地球深部过程. 地球科学，44(5)：1487-1493
庞振阵，夏明哲，王银强，满毅，夏昭德，张海东. 2025. 新疆北山启鑫岩体地幔源区性质及找矿启示：来自橄榄石成分的制约.

地质通报，44(10)：2003-2018
彭璐. 2023. 金川铜镍硫化物矿床西岩体地球化学特征及岩浆演化研究. 硕士学位论文. 长沙：中南大学
邱家骧，廖群安. 1996. 浙闽新生代玄武岩的岩石成因学与 Cpx 矿物化学. 火山地质与矿产，17(1-2)：16-25
冉凤琴，钟康惠，陆茂欣. 2015. 会理县力马河铜镍矿成矿要素及成矿模式研究. 四川有色金属，(4)：43-46
宋谢炎，侯增谦，曹志敏，卢纪仁，汪云亮，张成江，李佑国. 2001. 峨眉大火成岩省的岩石地球化学特征及时限. 地质学报，75(4)：498-506
汤中立，闫海卿，焦建刚，李小虎. 2006. 中国岩浆硫化物矿床新分类与小岩体成矿作用. 矿床地质，25(1)：1-9
汤中立，钱壮志，姜常义，闫海卿，焦建刚，刘民武，徐章华，徐刚，王亚磊. 2011. 岩浆硫化物矿床勘查研究的趋势与小岩体成矿系统. 地球科学与环境学报，33(1)：1-9
陶琰，胡瑞忠，漆亮，罗泰义. 2007. 四川力马河镁铁-超镁铁质岩体的地球化学特征及成岩成矿分析. 岩石学报，23(11)：2785-2800
陶琰，胡瑞忠，屈文俊，杜安道. 2008. 力马河镍矿 Re-Os 同位素研究. 地质学报，82(9)：1292-1304
王良果. 2015. 云南省金宝山基性—超基性杂岩体特征及找矿远景. 硕士学位论文. 成都：成都理工大学
王萌，张招崇，侯通，骆文娟. 2011. 攀西地区大板山岩体的年代学、元素地球化学及其对铜镍硫化物矿床成因的约束. 岩石学报，27(9)：2665-2678
王焰. 2008. 云南二叠纪白马寨铜镍硫化物矿床的成因：地壳混染与矿化的关系. 矿物岩石地球化学通报，27(4)：332-343
徐文博. 2023. 北山启鑫镁铁-超镁铁质杂岩体镍钴成矿岩浆作用——C-He-Ne-Ar 同位素制约. 硕士学位论文. 兰州：兰州大学
徐章华，汤中立，蔡克勤. 1998. 金川铜、镍(含 PGE)岩浆硫化物矿床母岩浆成分的估计. 现代地质，12(4)：506-514
姚家栋. 1988. 西昌地区硫化铜(铂)镍矿床成因. 重庆：重庆出版社
尤敏鑫，张照伟，刘建民，张江伟，王亚磊，钱兵. 2017. 攀西地区镁铁-超镁铁岩地球化学与岩浆型 Cu-Ni-(PGE)硫化物矿床成矿. 西北地质，50(3)：146-161
张飞飞. 2023. 夏日哈木镍钴硫化物矿床多期次成岩成矿作用研究. 硕士学位论文. 合肥：合肥工业大学
张磊，任钟元，张乐. 2022. 峨眉山大火成岩省平川苦橄岩地幔源区性质——来自橄榄石微量元素的制约. 大地构造与成矿学，46(1)：112-131
张云湘. 1982. 中国西南部一个南北向重要地质构造单元"攀枝花-西昌裂谷带". 四川地质学报，3(增1)：11-24，58
张照伟，王亚磊，邵继，李文渊. 2021. 东昆仑夏日哈木超大型岩浆镍钴硫化物矿床成矿特征. 矿床地质，40(6)：1230-1247
张志炳，李文渊，张照伟，刘月高，钱兵，王亚磊，张江伟，王博林，张洪川. 2016. 东昆仑夏日哈木岩浆铜镍硫化物矿床铬尖晶石特征及其指示意义. 矿物岩石地球化学通报，35(5)：966-975
赵冰冰，邓宇峰，周涛发，袁峰，张达玉，邓刚，李卫东，李跃. 2018. 东天山白鑫滩含铜镍矿镁铁-超镁铁岩体的岩石成因：年代学、岩石地球化学和 Sr-Nd 同位素证据. 岩石学报，34(9)：2733-2753
赵瑛. 2020. 峨眉山大火成岩省攀枝花基性-超基性岩墙成因研究. 硕士学位论文. 兰州：兰州大学
钟祥. 2019. "攀枝花式"钒钛磁铁矿矿床成矿机制研究. 硕士学位论文. 成都：西南石油大学
朱飞霖，白梅，陶琰. 2017. 攀西小关河地区核桃树富铂岩浆硫化物矿床岩石地球化学特征及成矿机制研究. 岩石学报，33(7)：2225-2240